Supporting Information

Functionalized Guanidinium Chloride Based Colourimetric Sensors for Fluoride and Acetate: Single Crystal X-ray Structural Evidence of -NH Deprotonation and Complexation

Purnandhu Bose, Nisar B. Ahamed and Pradyut Ghosh*

Department of Inorganic Chemistry, Indian Association for the Cultivation of Science, 2A & 2B Raja S. C. Mullick Road, Kolkata 700032, India.E-mail: icpg@iacs.res.in

Contents **Page No.**

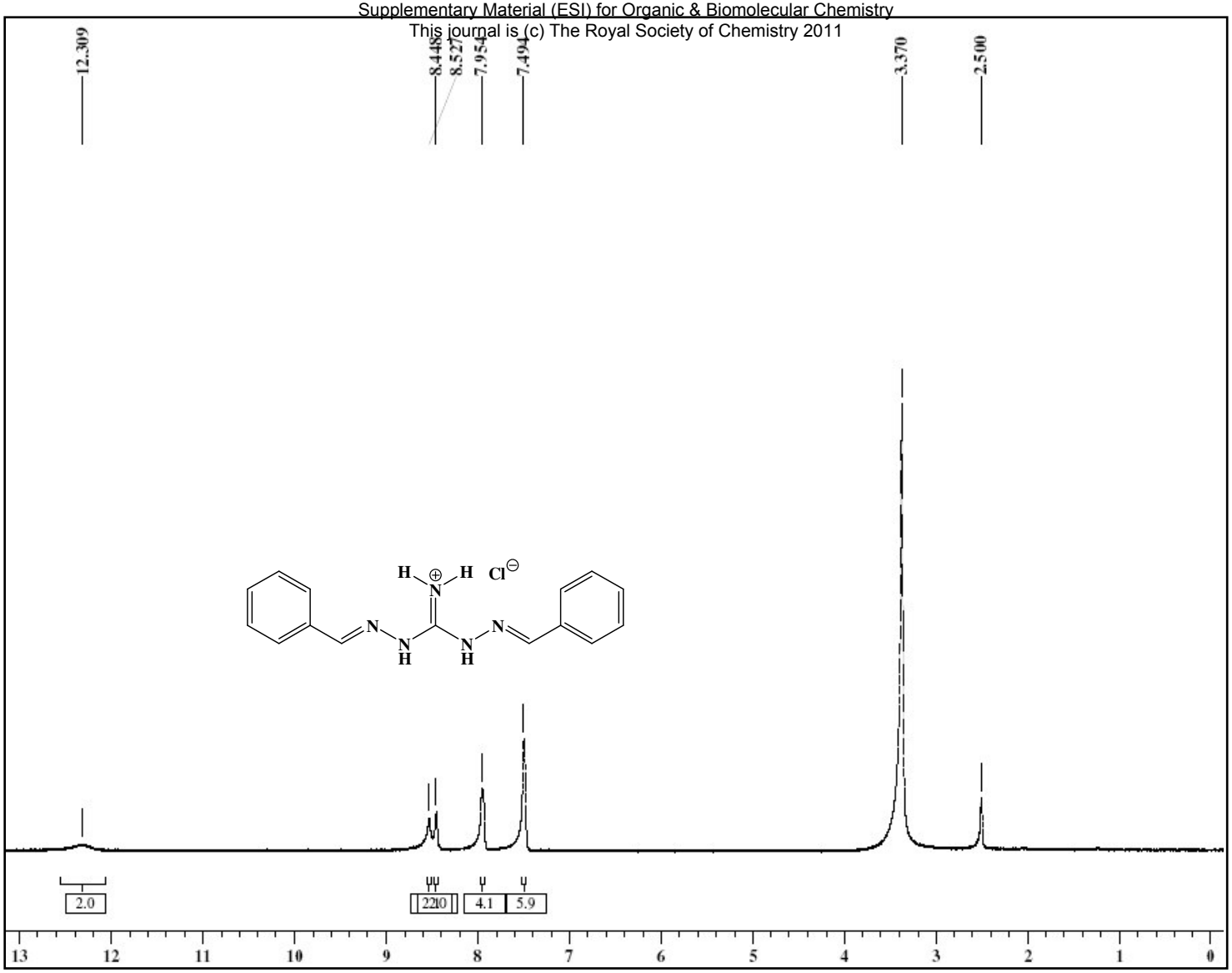

Figure S1. ^{1}H NMR spectrum of **S1** in DMSO-d_6.

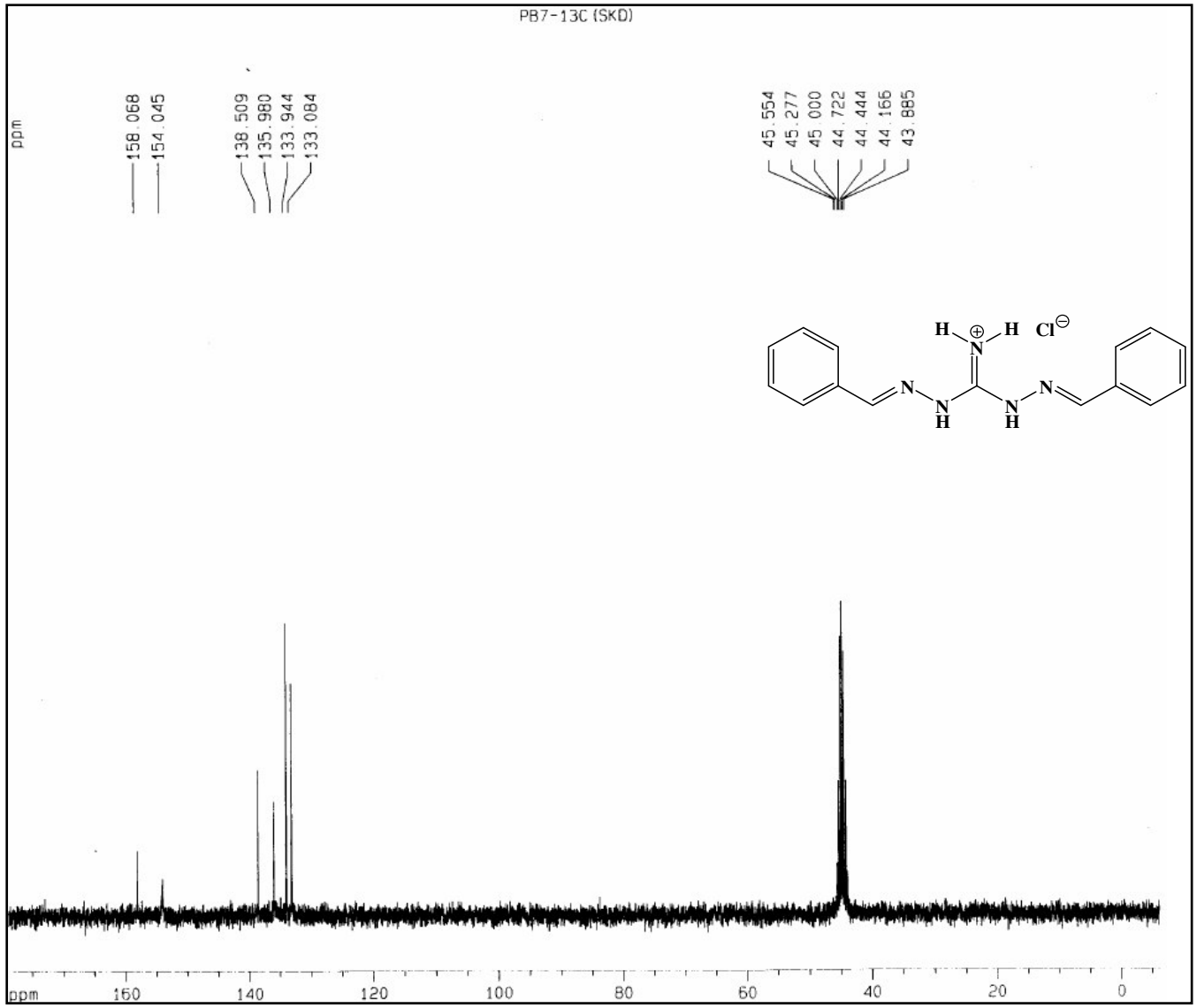

Figure S2. ^{13}C NMR spectrum of **S1** in DMSO-d_6.

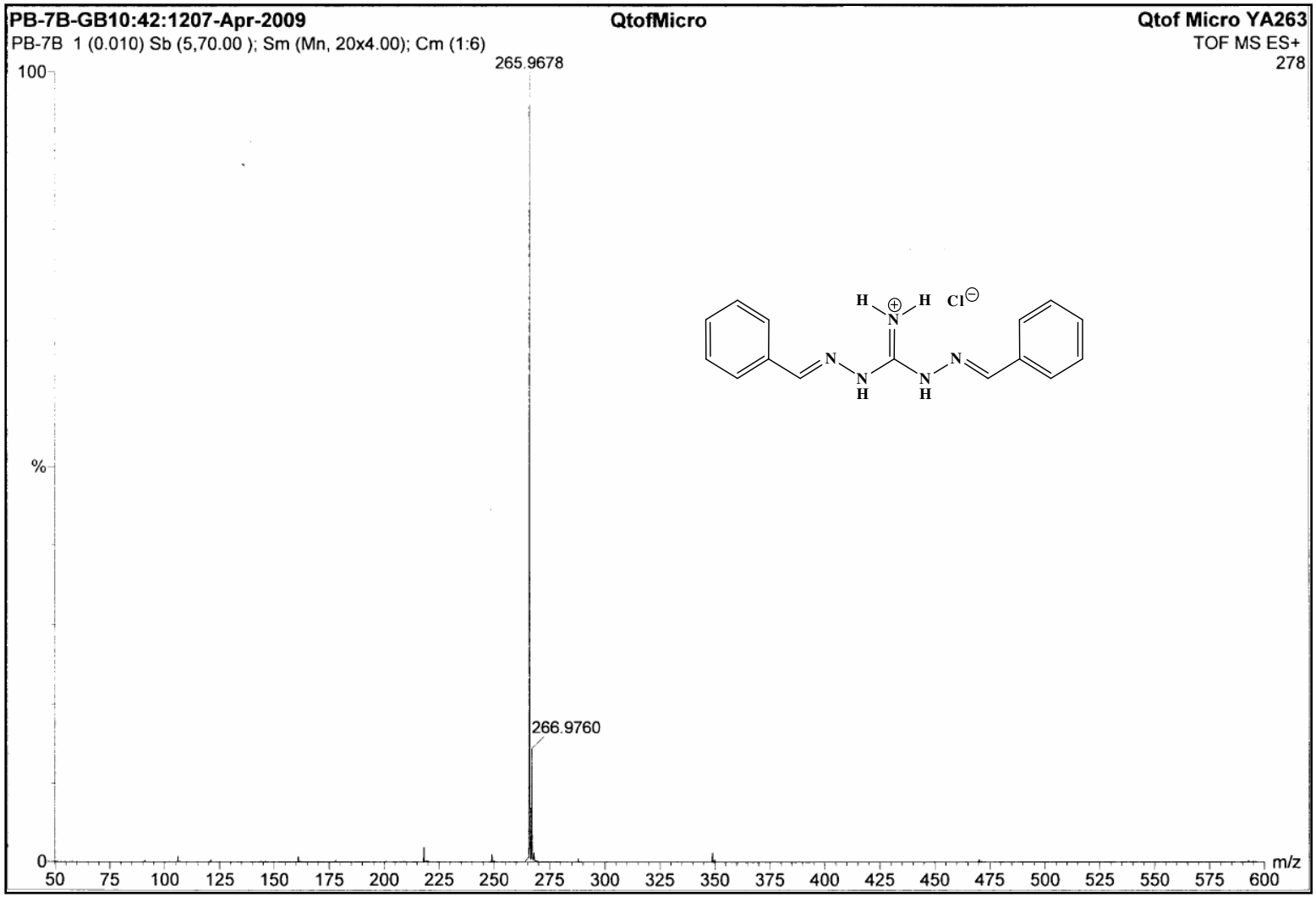

Figure S3. HRMS spectrum of **S1**.

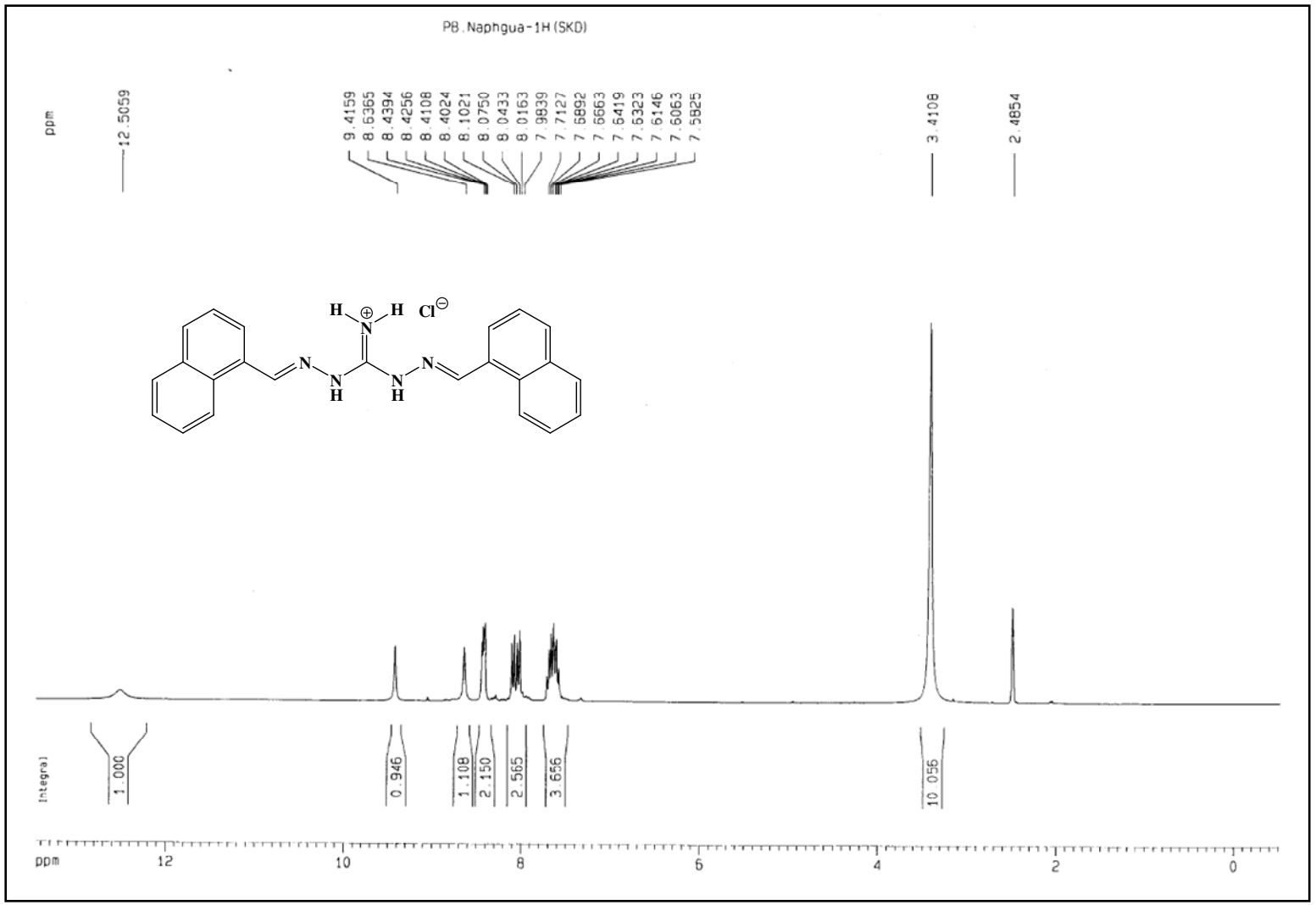

Figure S4. ^{1}H NMR spectrum of **S2** in DMSO-d_6.

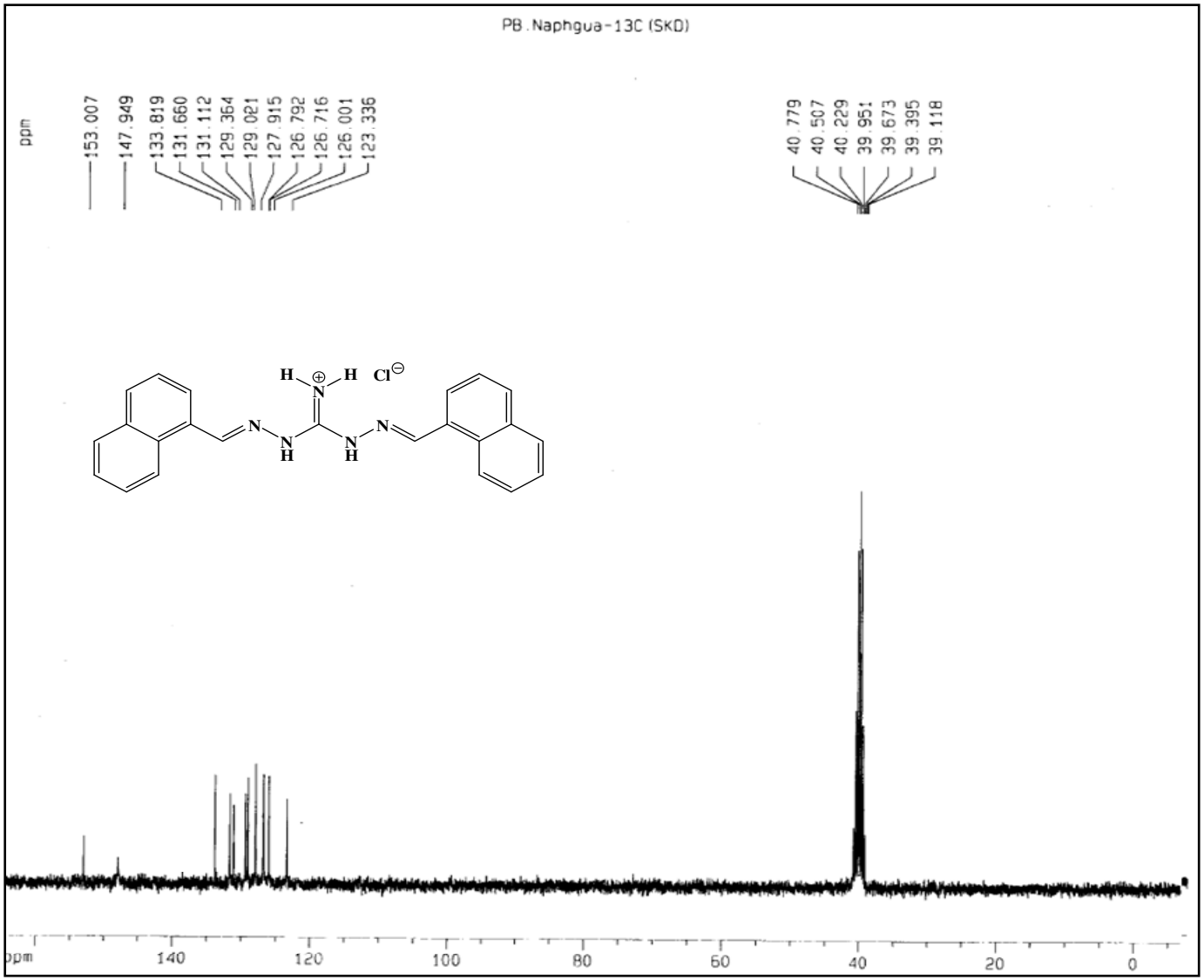

Figure S5. ^{13}C NMR spectrum of **S2** in DMSO-d_6.

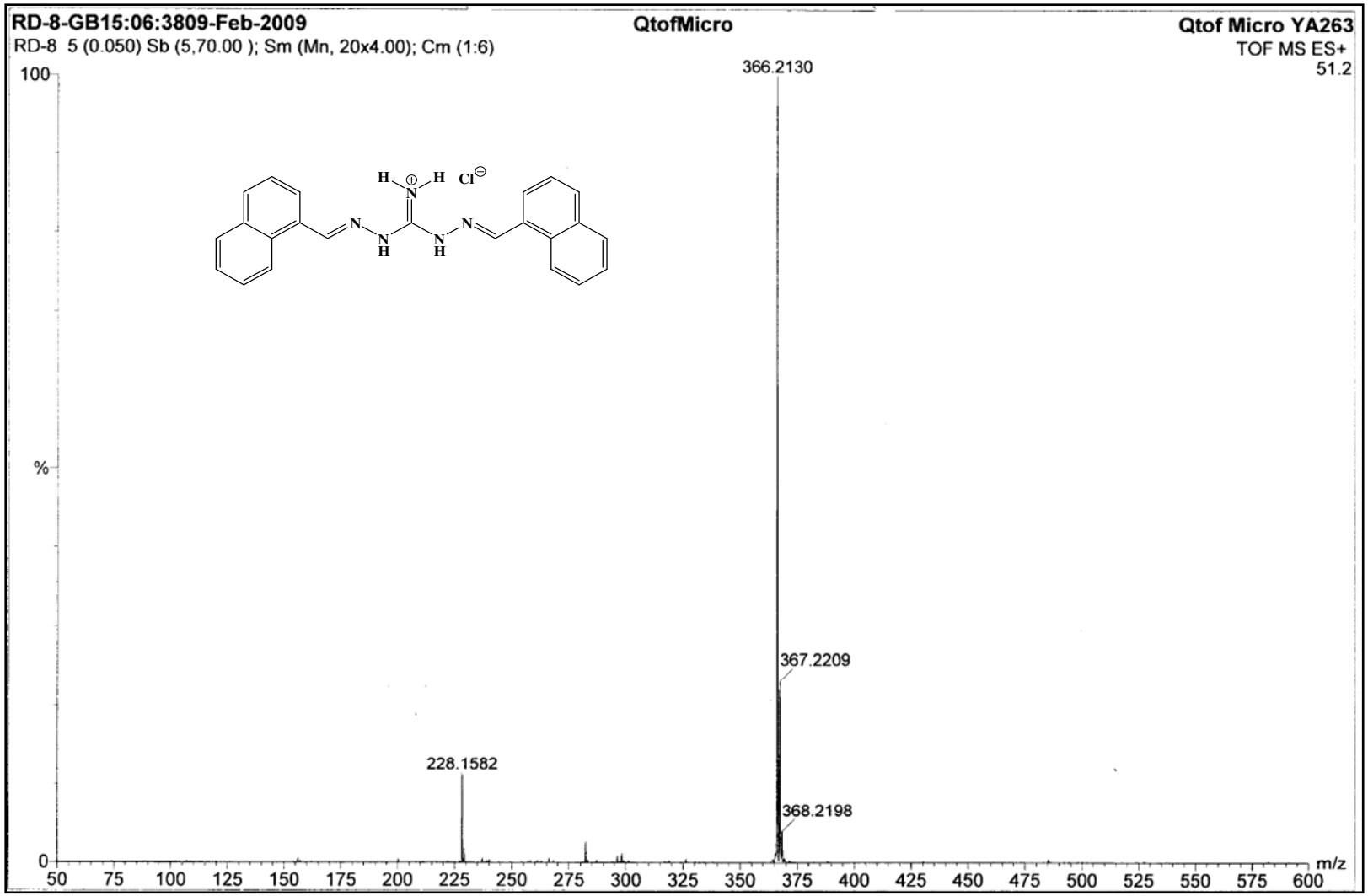

Figure S6. HRMS spectrum of **S2**.

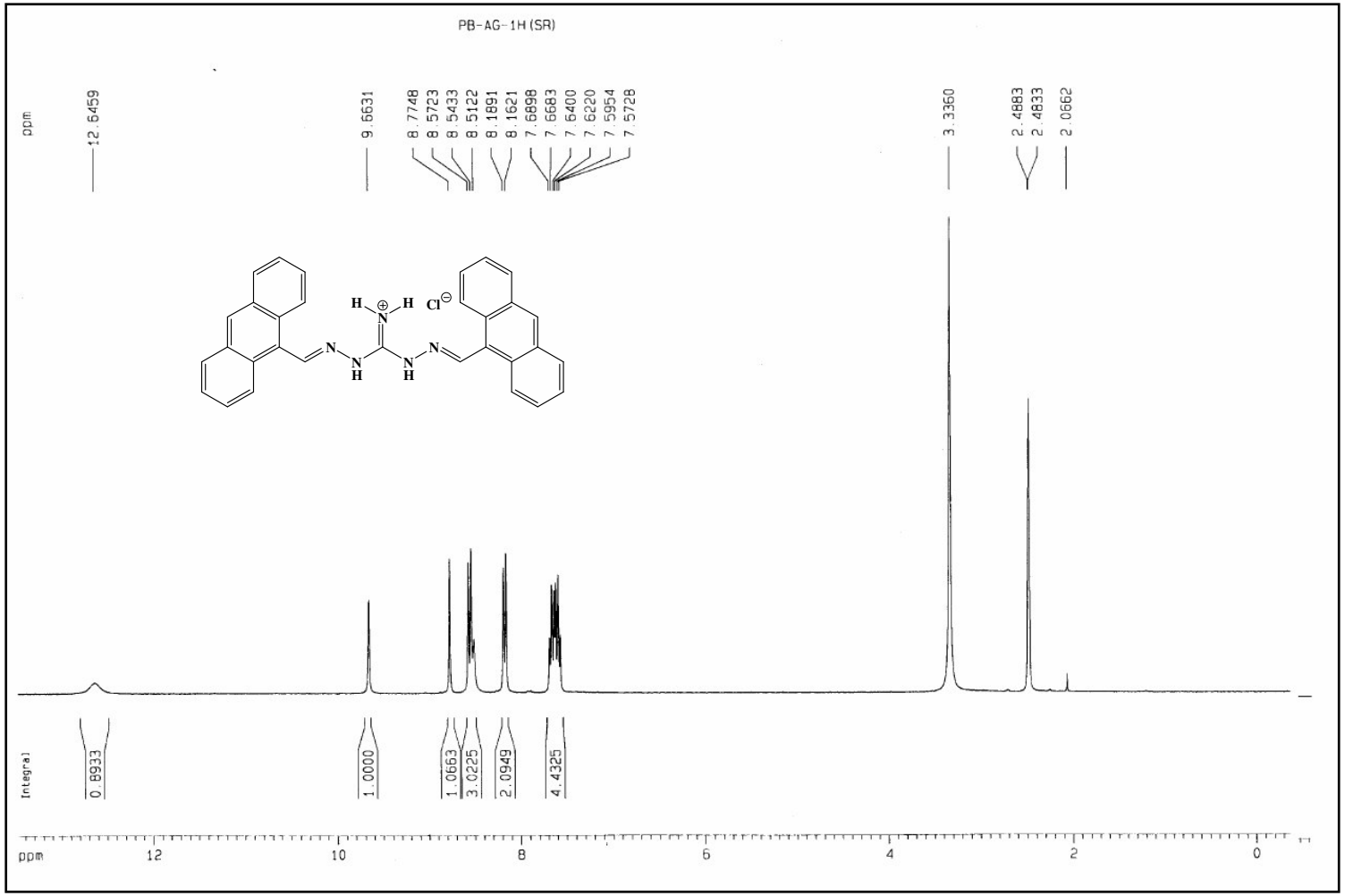

Figure S7. ^{1}H NMR spectrum of **S3** in DMSO-d_6.

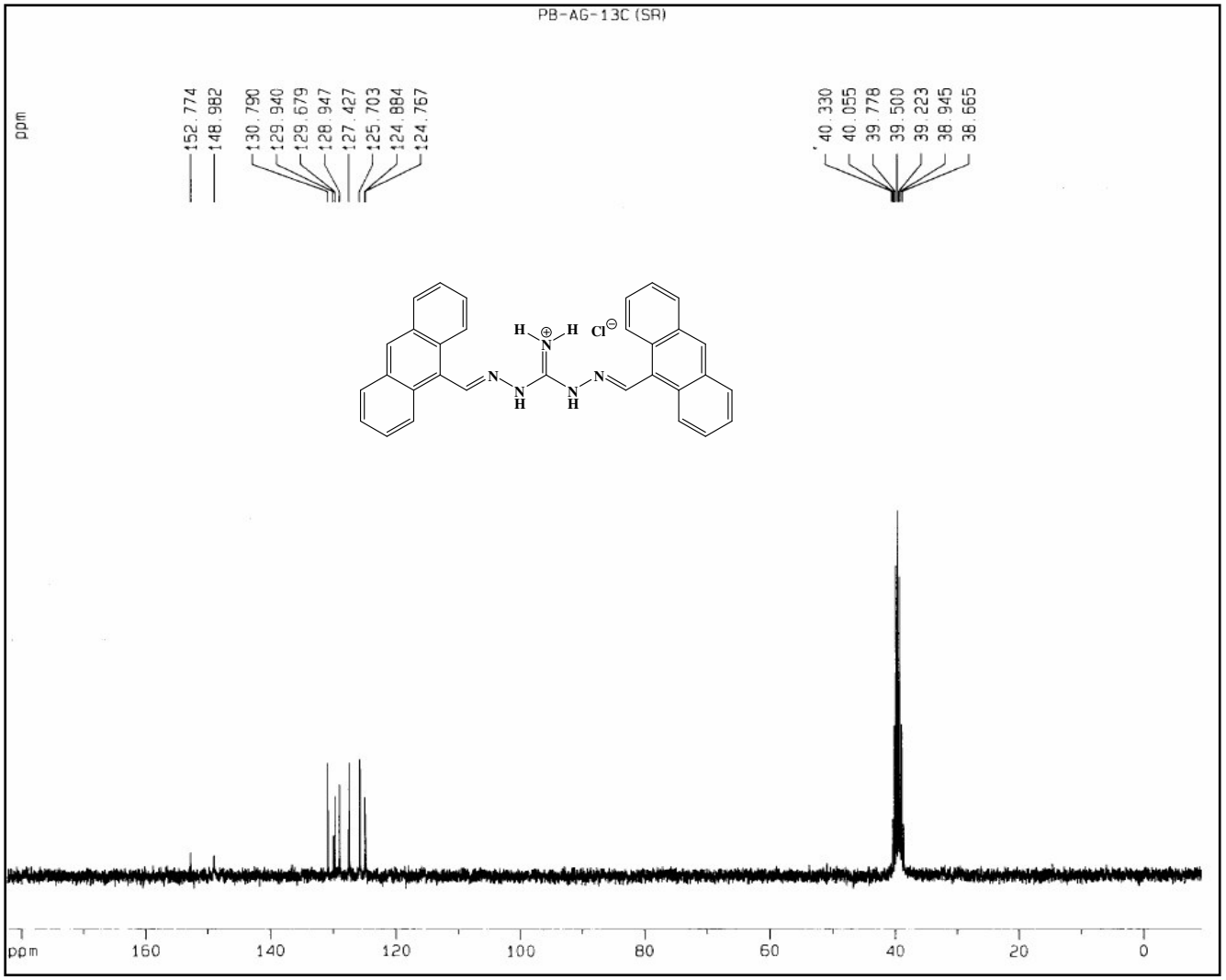

Figure S8. ^{13}C NMR spectrum of **S3** in DMSO-d_6.

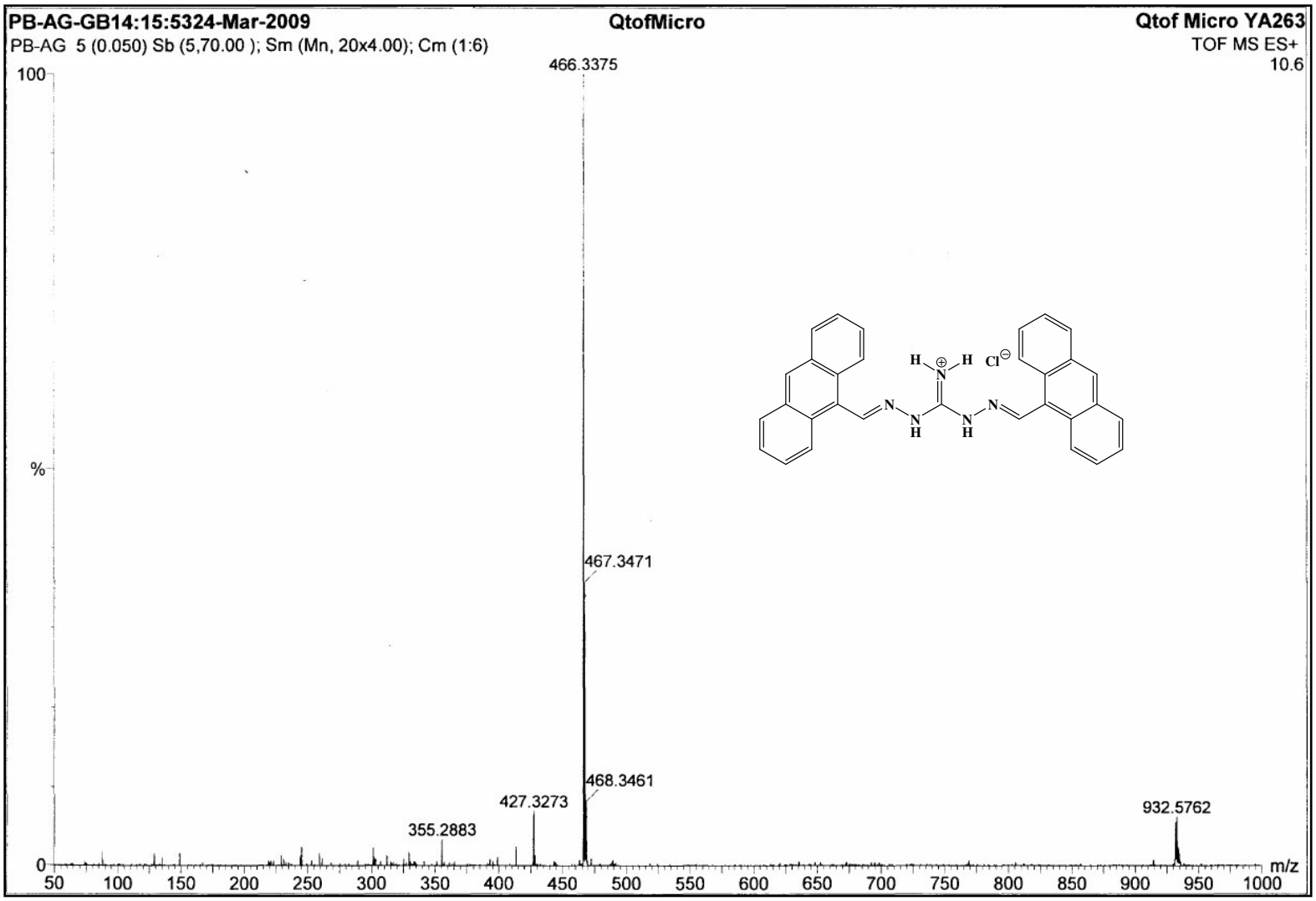

Figure S9. HRMS spectrum of **S3**.

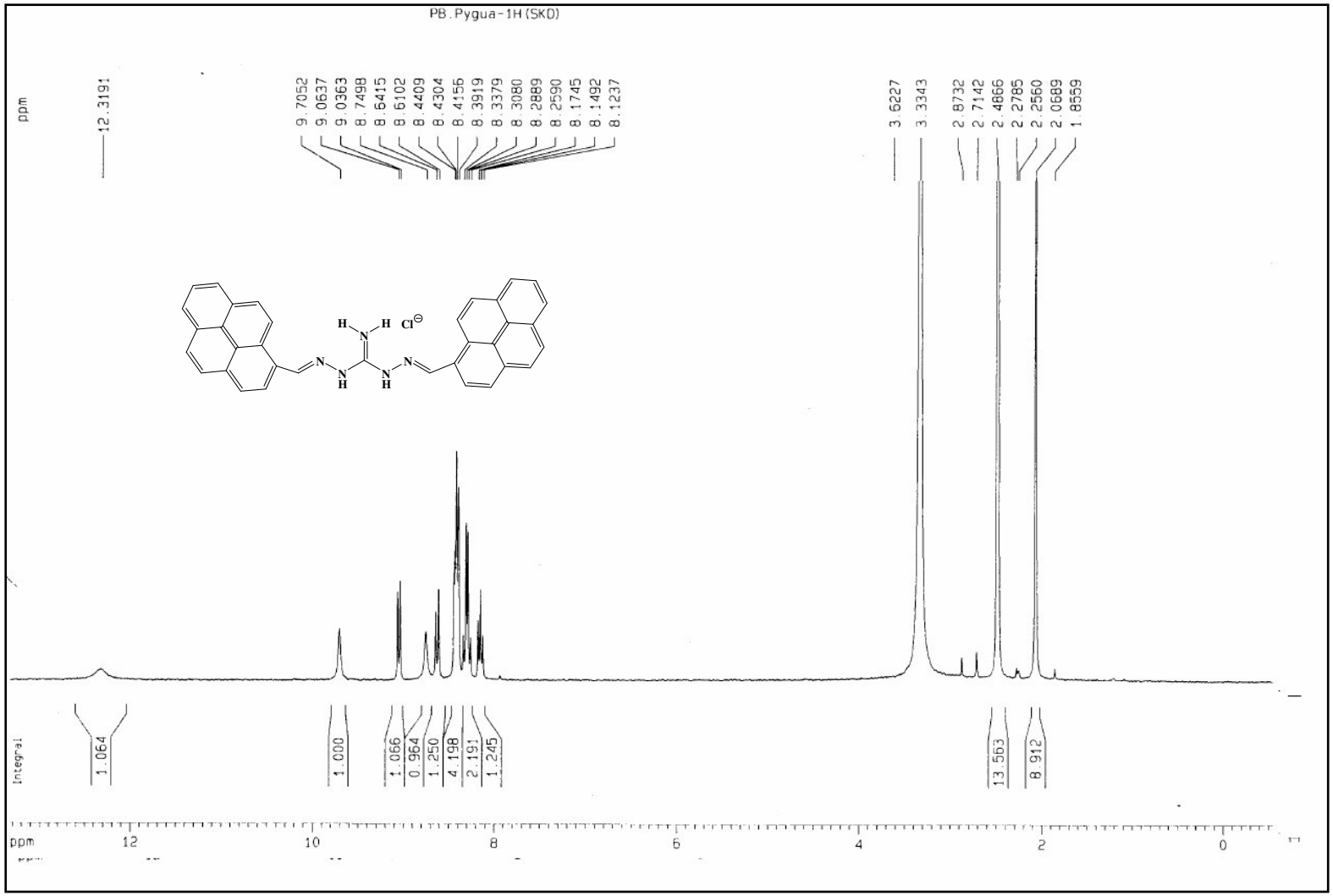

Figure S10. ^{1}H NMR spectrum of **S4** in DMSO-d_6.

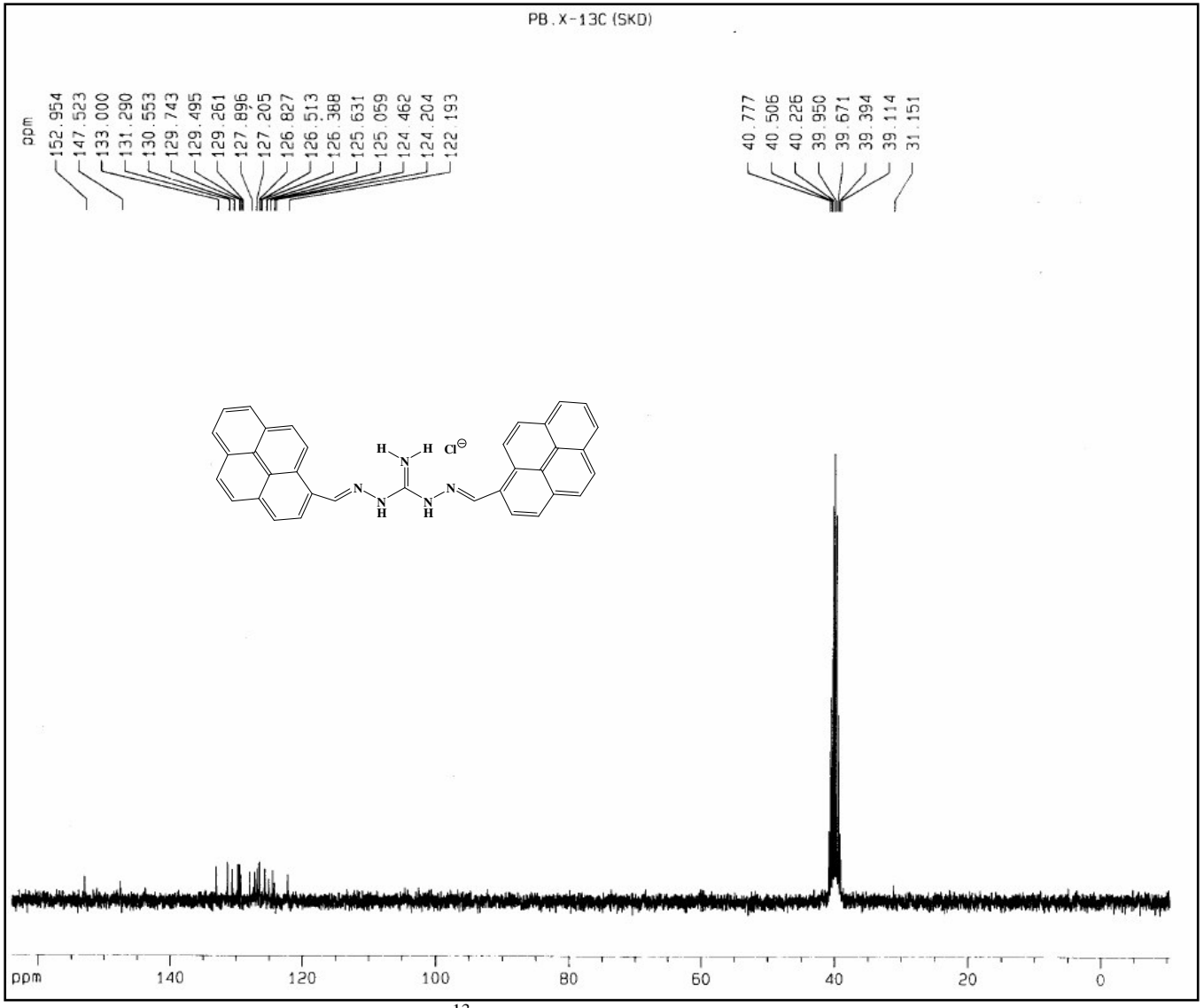

Figure S11. ^{13}C NMR spectrum of **S4** in DMSO-d_6.

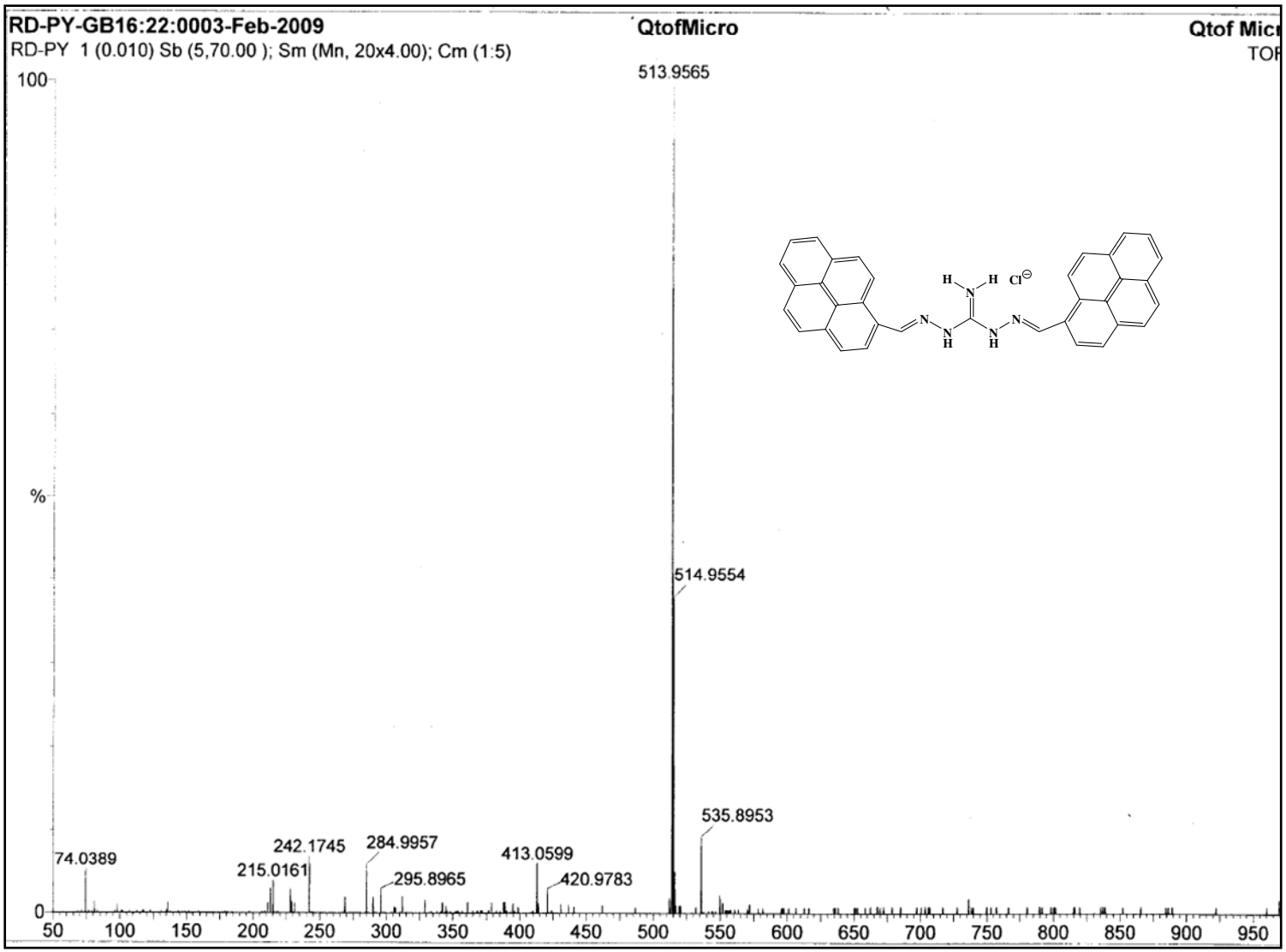

Figure S12. HRMS spectrum of **S4**.

Figure S13. ^{1}H NMR spectrum of **S5** in DMSO-d_6.

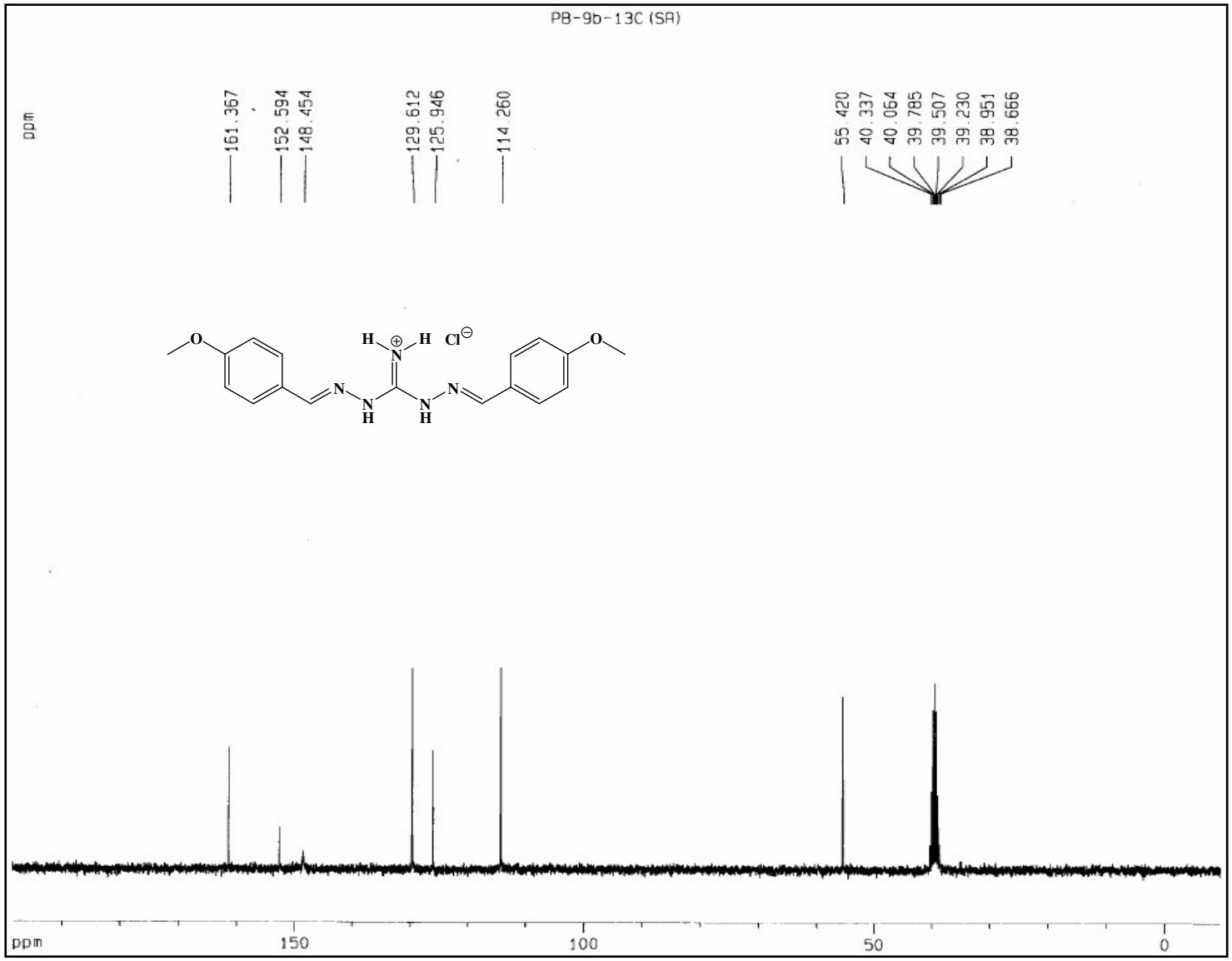

Figure S14. ^{13}C NMR spectrum of **S5** in DMSO-d_6.

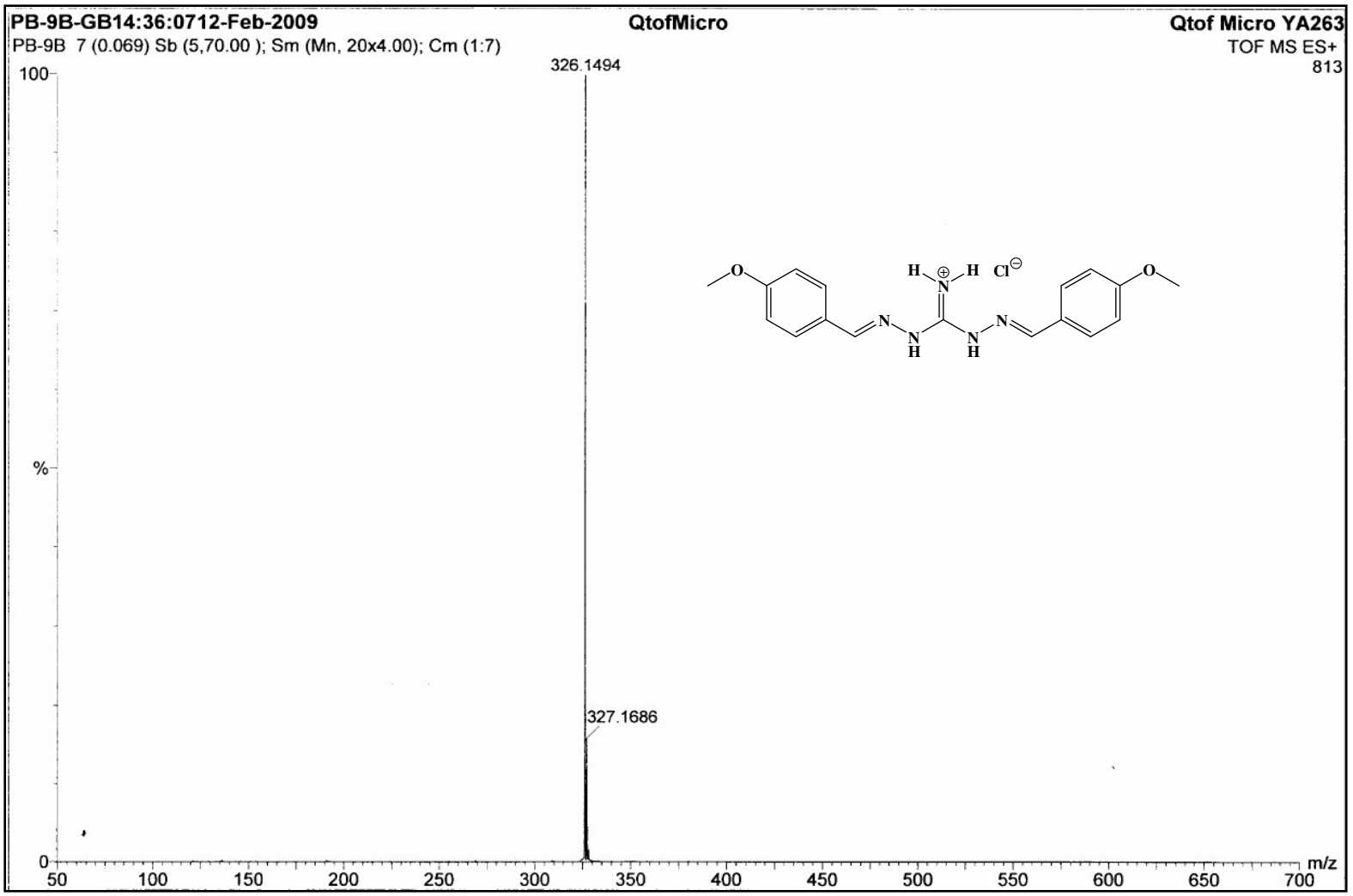

Figure S15. HRMS spectrum of **S5**.

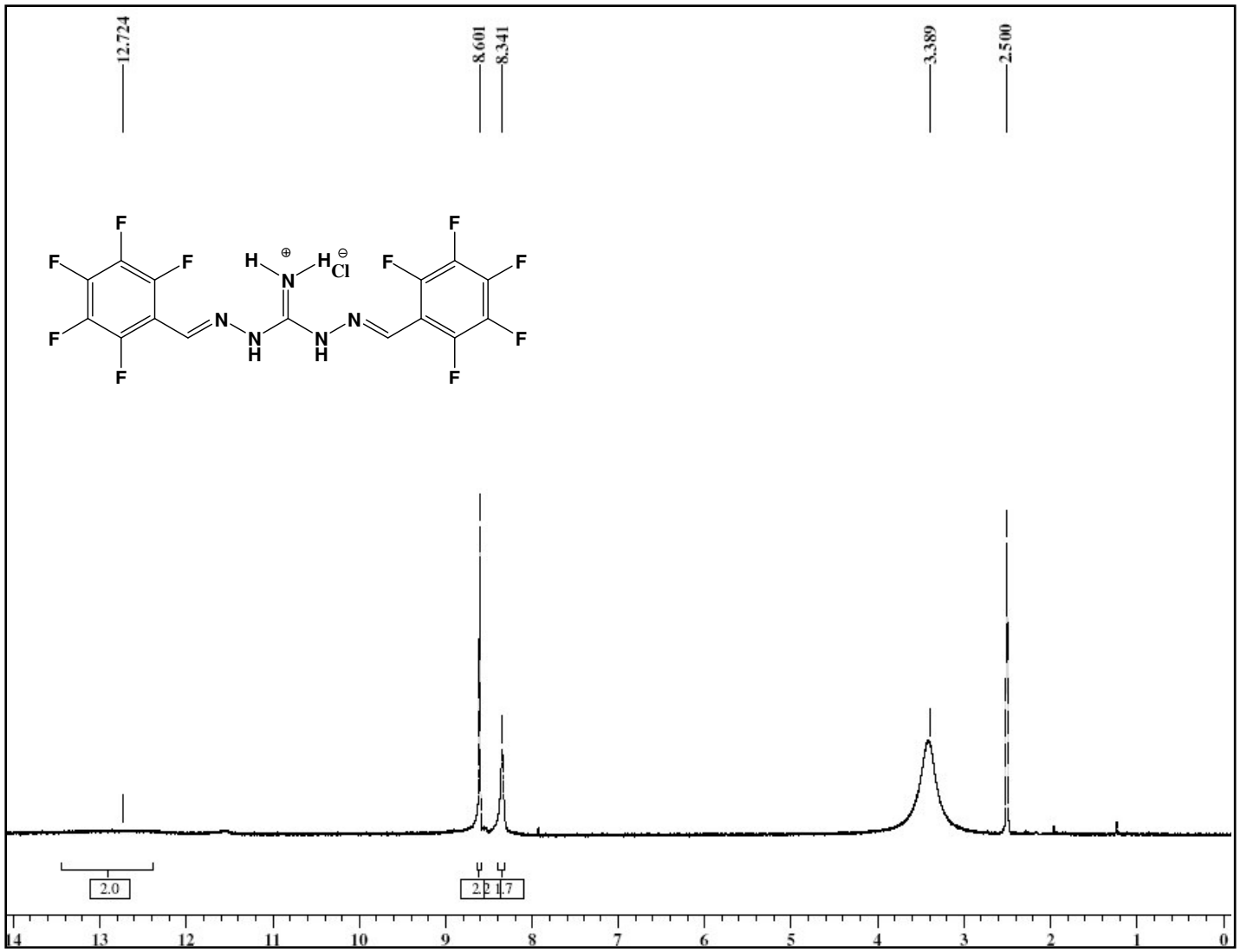

Figure S16. ^{1}H NMR spectrum of **S6** in DMSO-d_6.

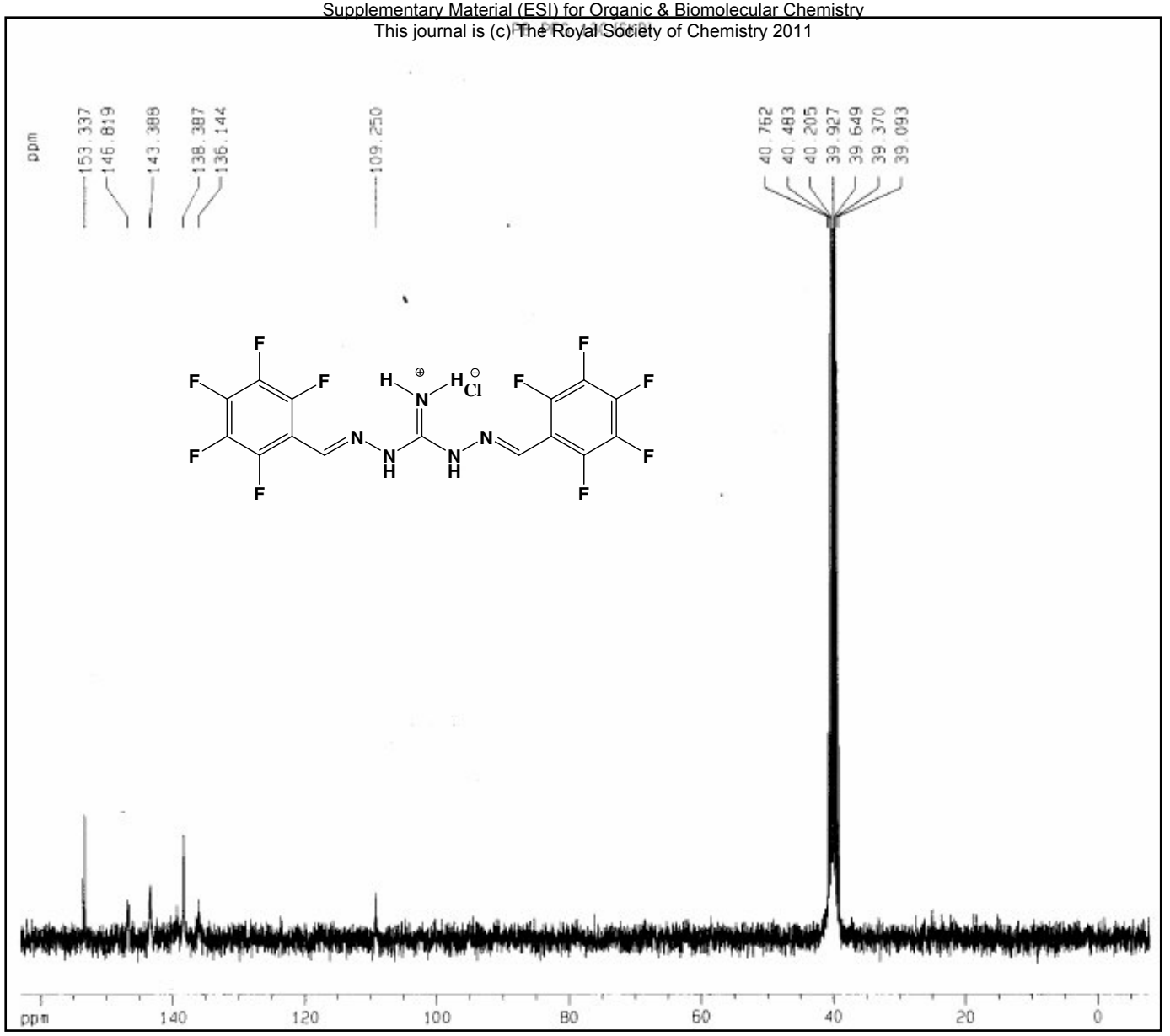

Figure S17. ^{13}C NMR spectrum of **S6** in DMSO-d_6.

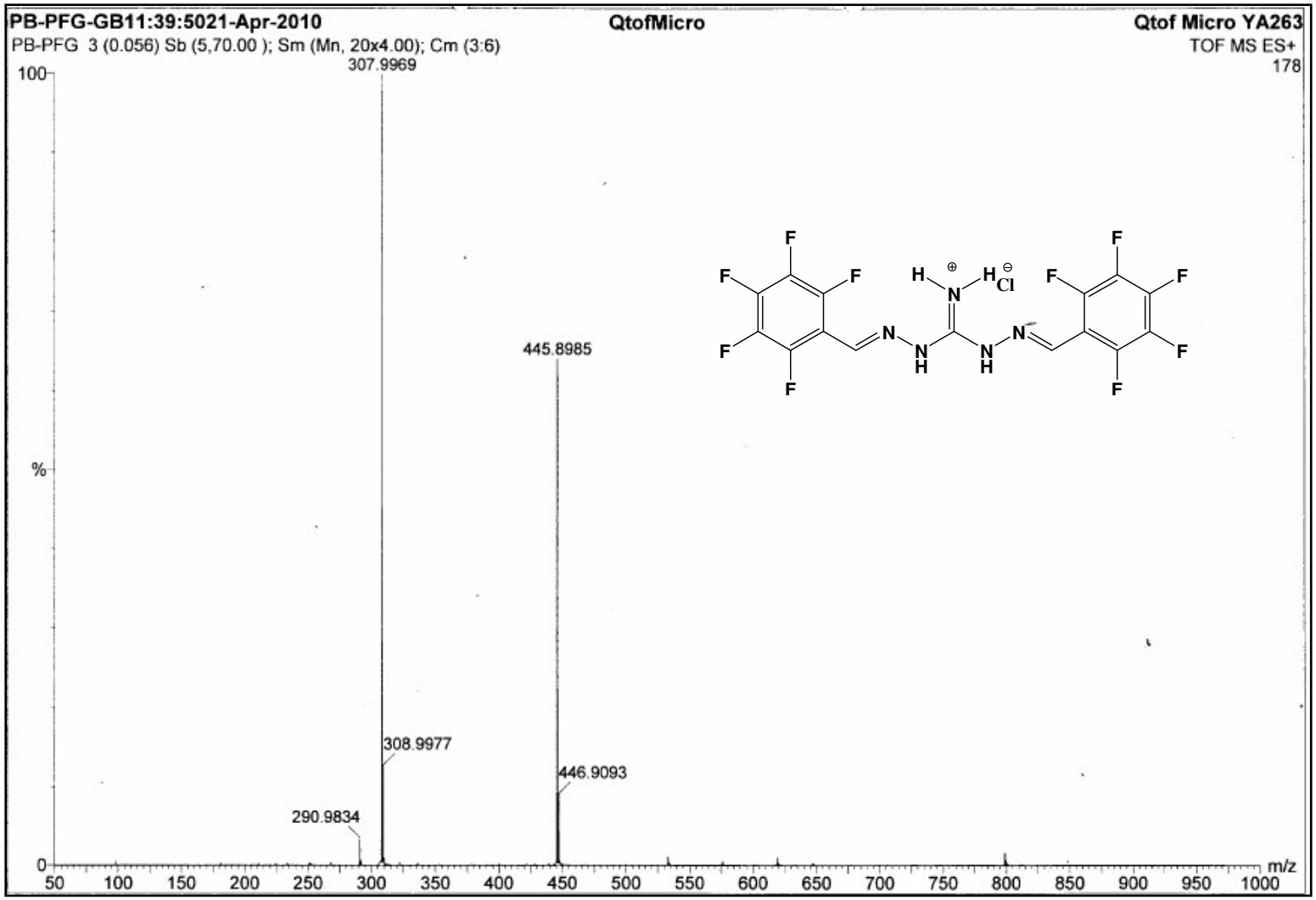

Figure S18. HRMS spectrum of **S6**.

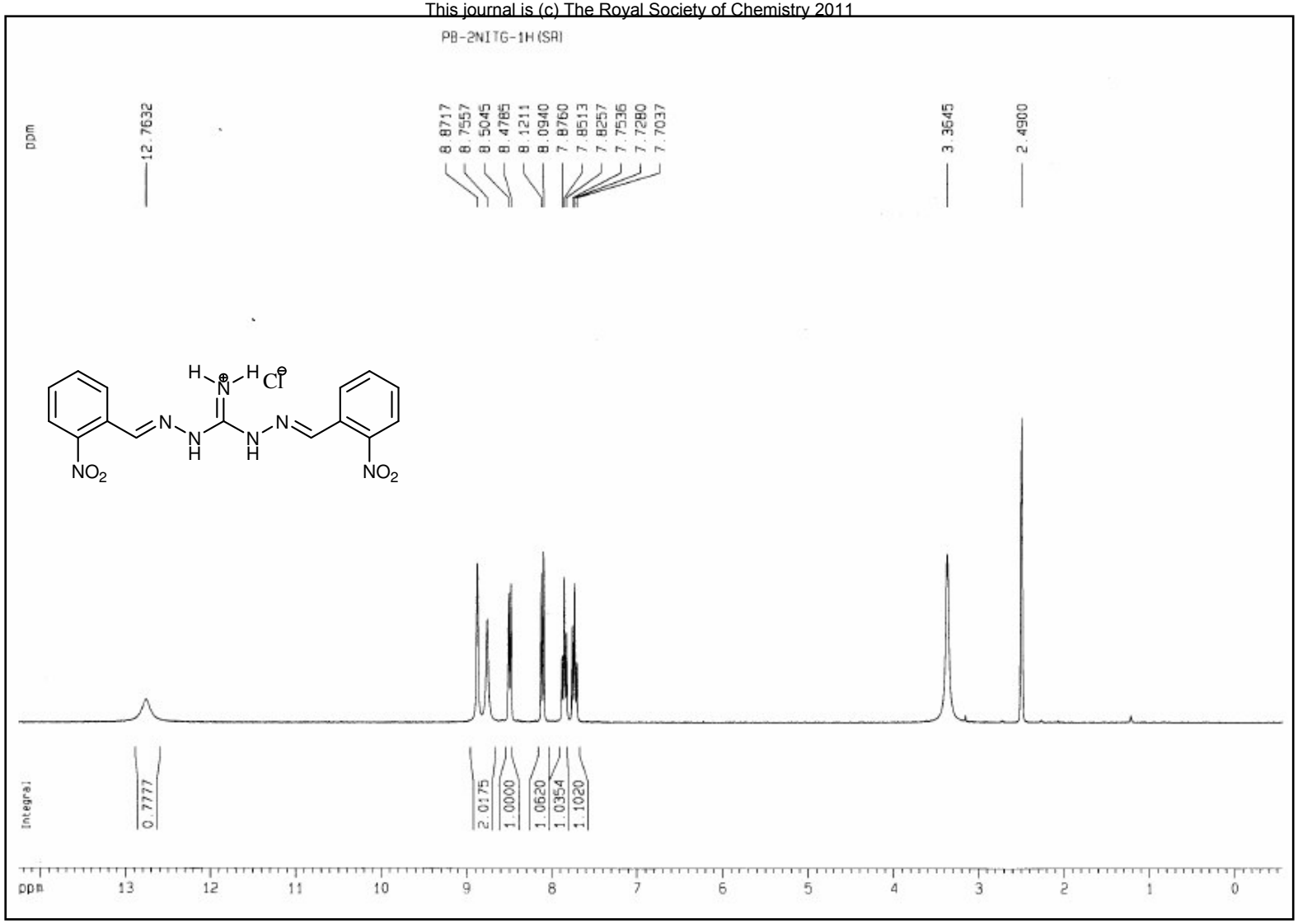

Figure S19. ^{1}H NMR spectrum of **S7** in DMSO-d_6.

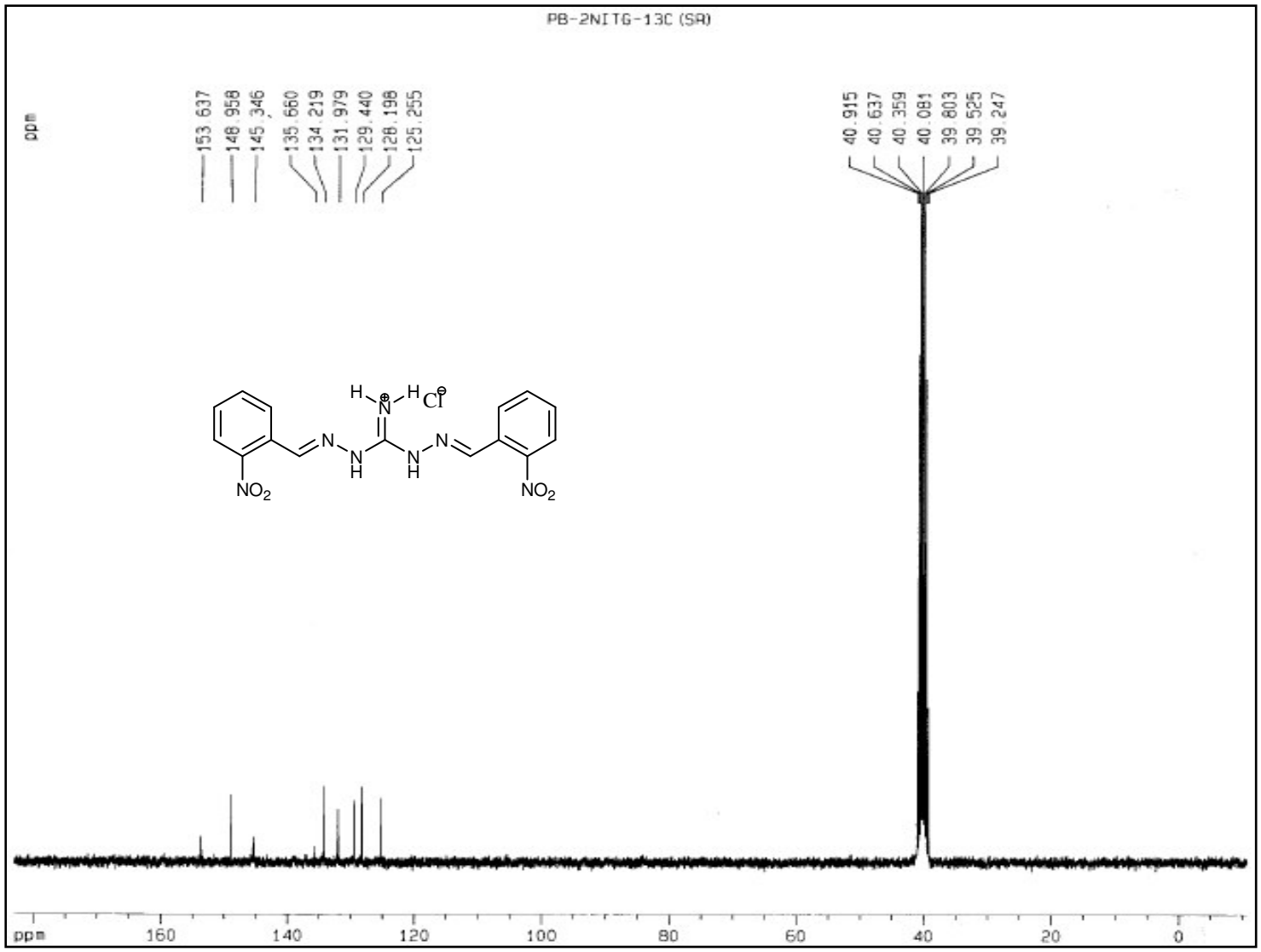

Figure S20. ^{13}C NMR spectrum of **S7** in DMSO-d_6.

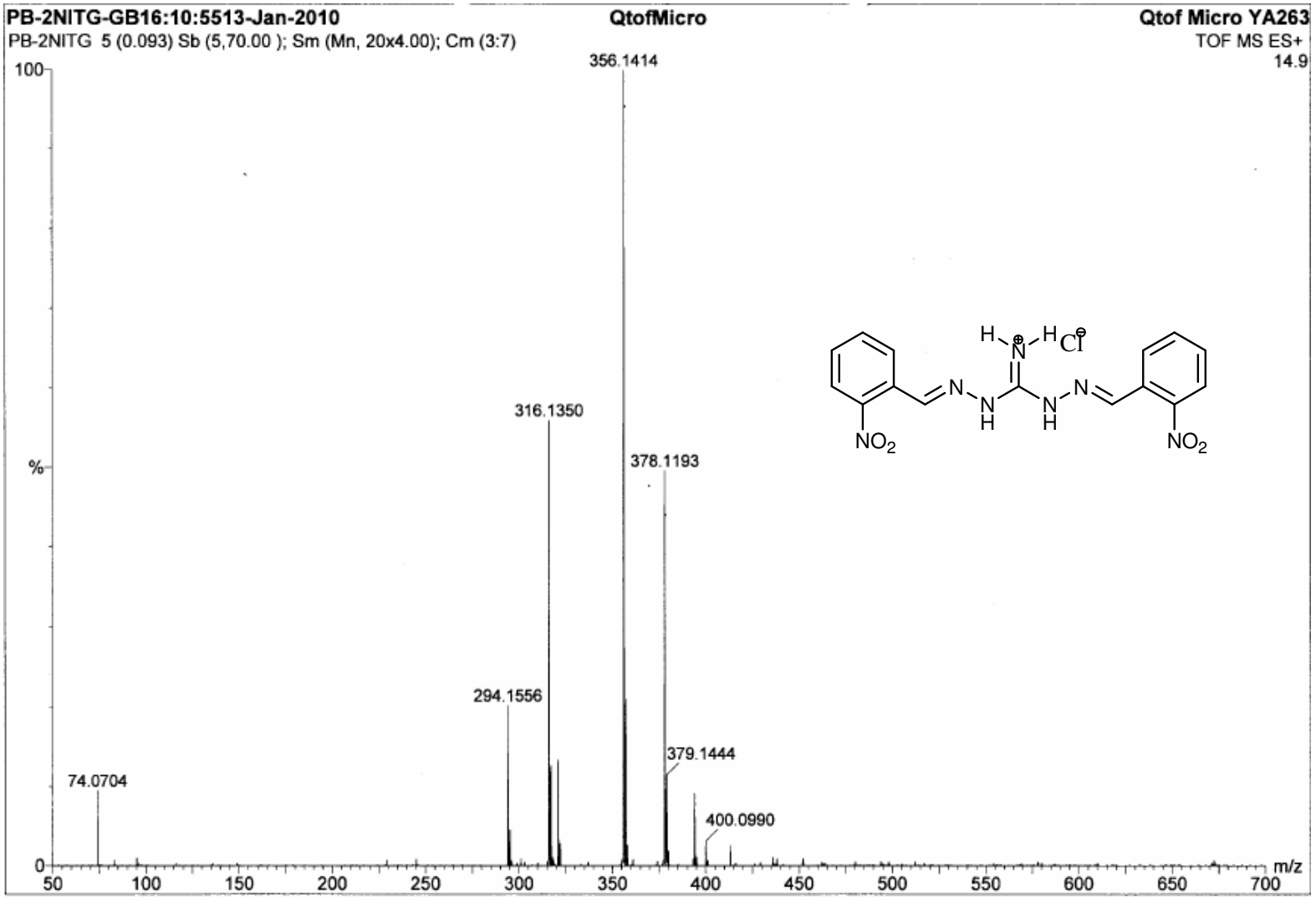

Figure S21. HRMS spectrum of **S7**.

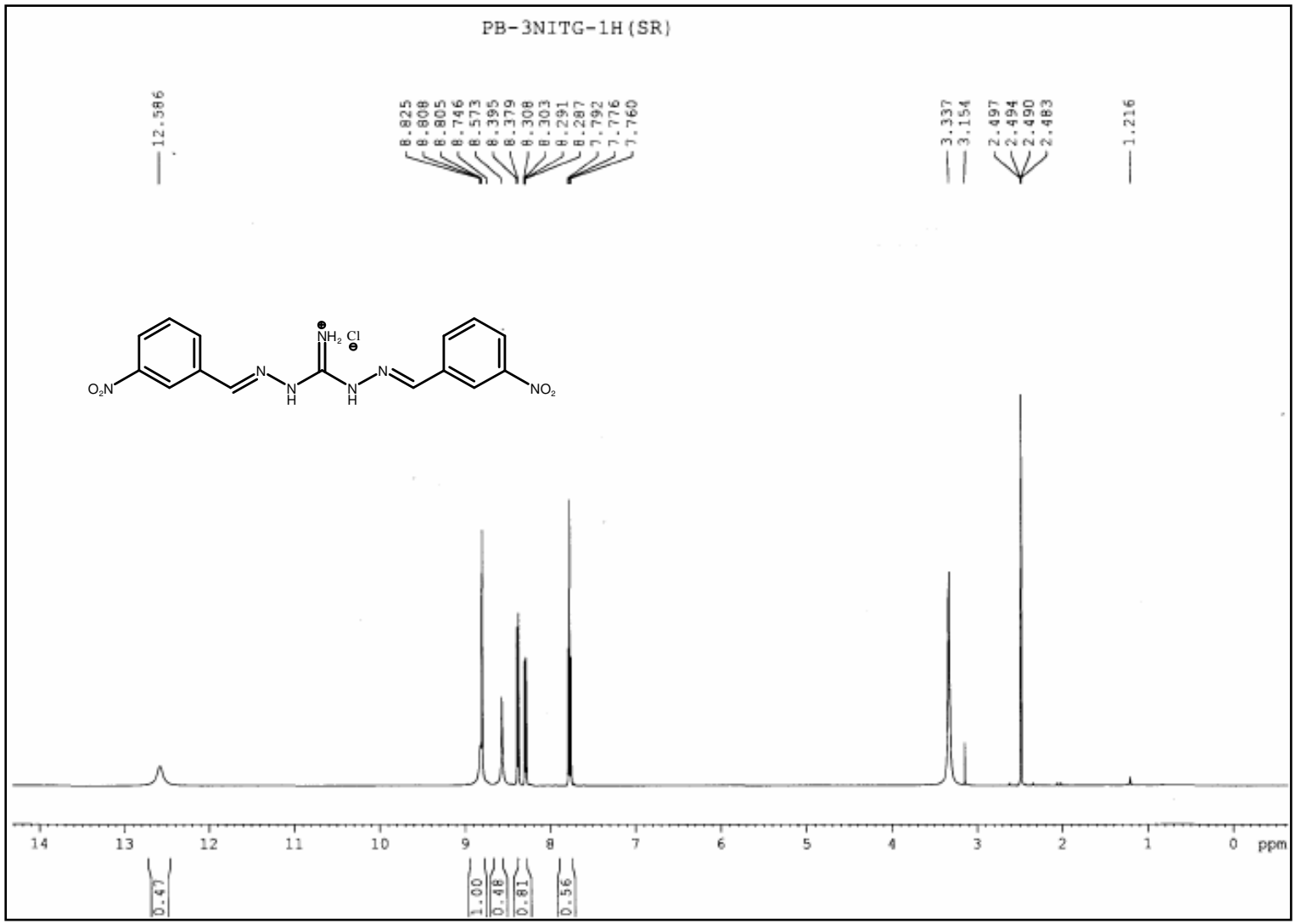

Figure S22. ^{1}H NMR spectrum of **S8** in DMSO-d_6.

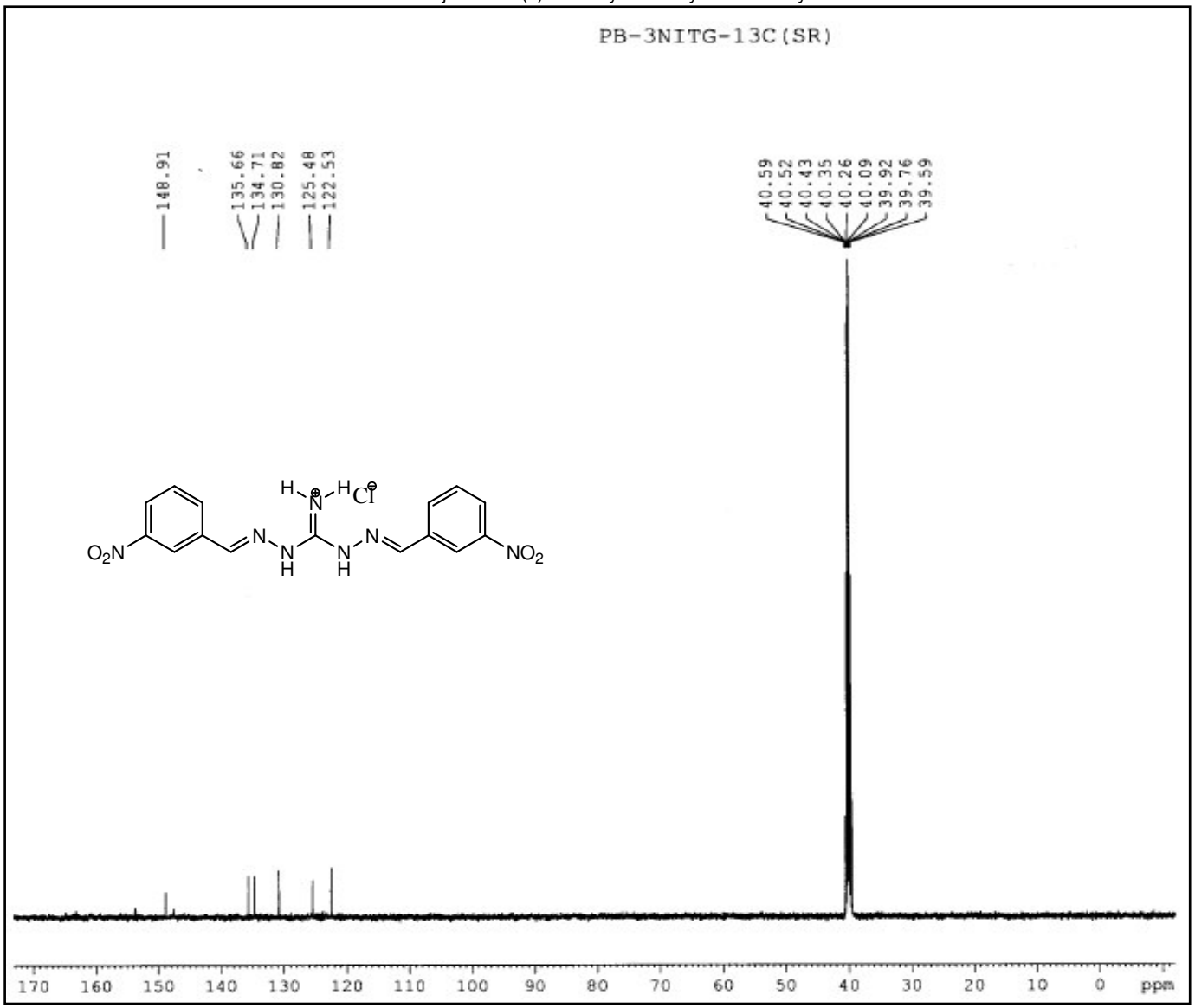

Figure S23. ^{13}C NMR spectrum of **S8** in DMSO-d_6.

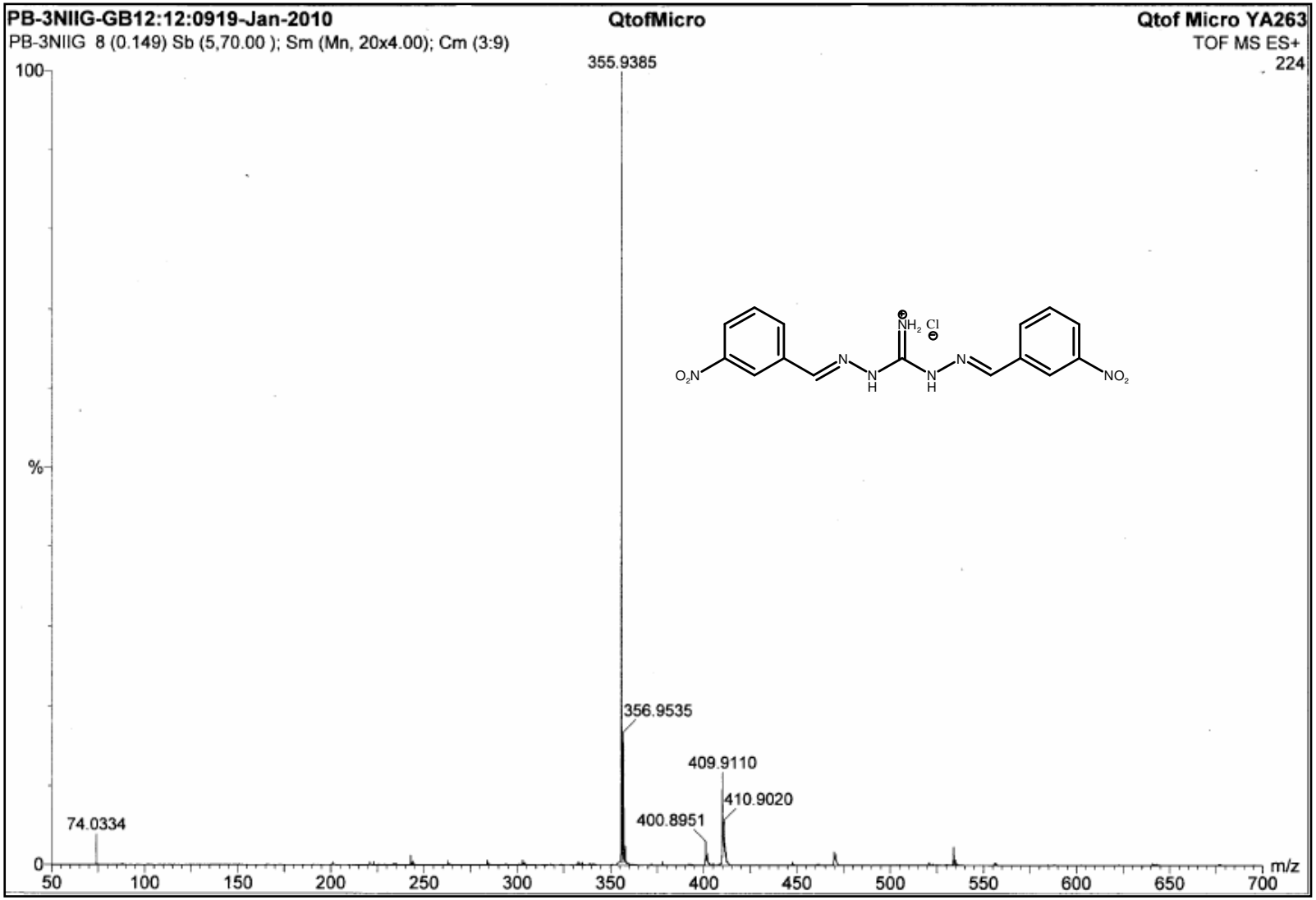

Figure S24. HRMS spectrum of **S8**.

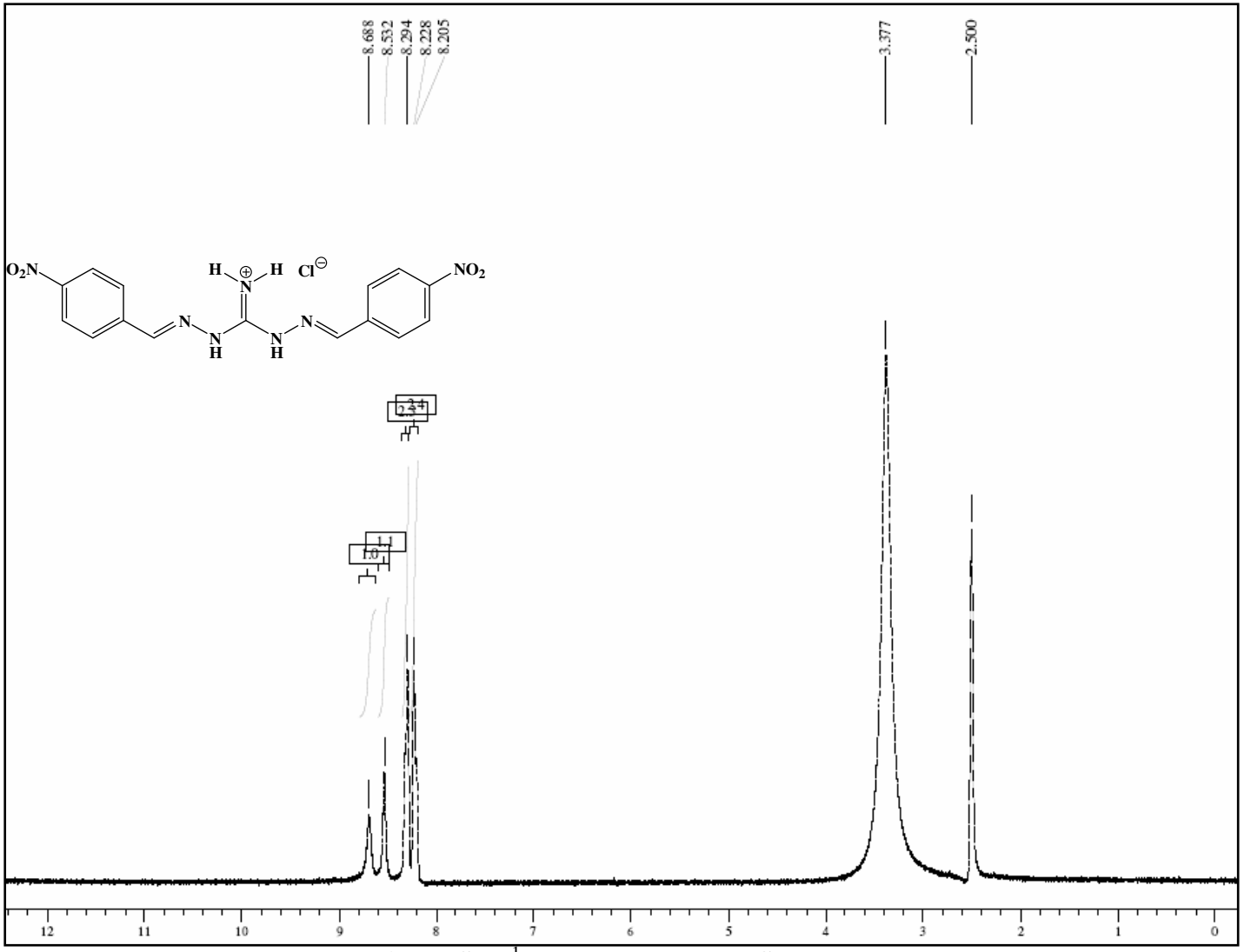

Figure S25. ^{1}H NMR spectrum of **S9** in DMSO-d_{6}.

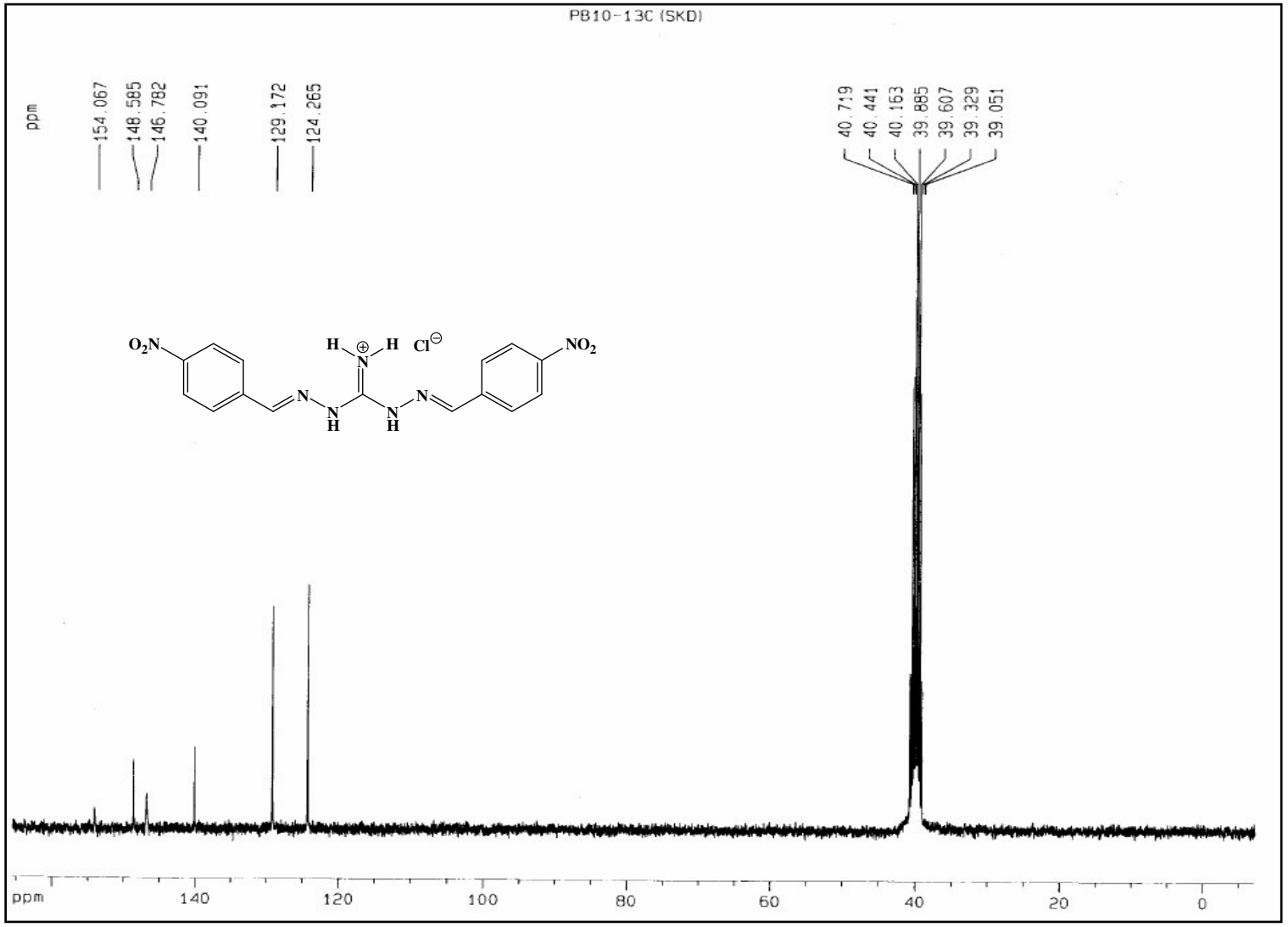

Figure S26. ^{13}C NMR spectrum of **S9** in DMSO-d_6.

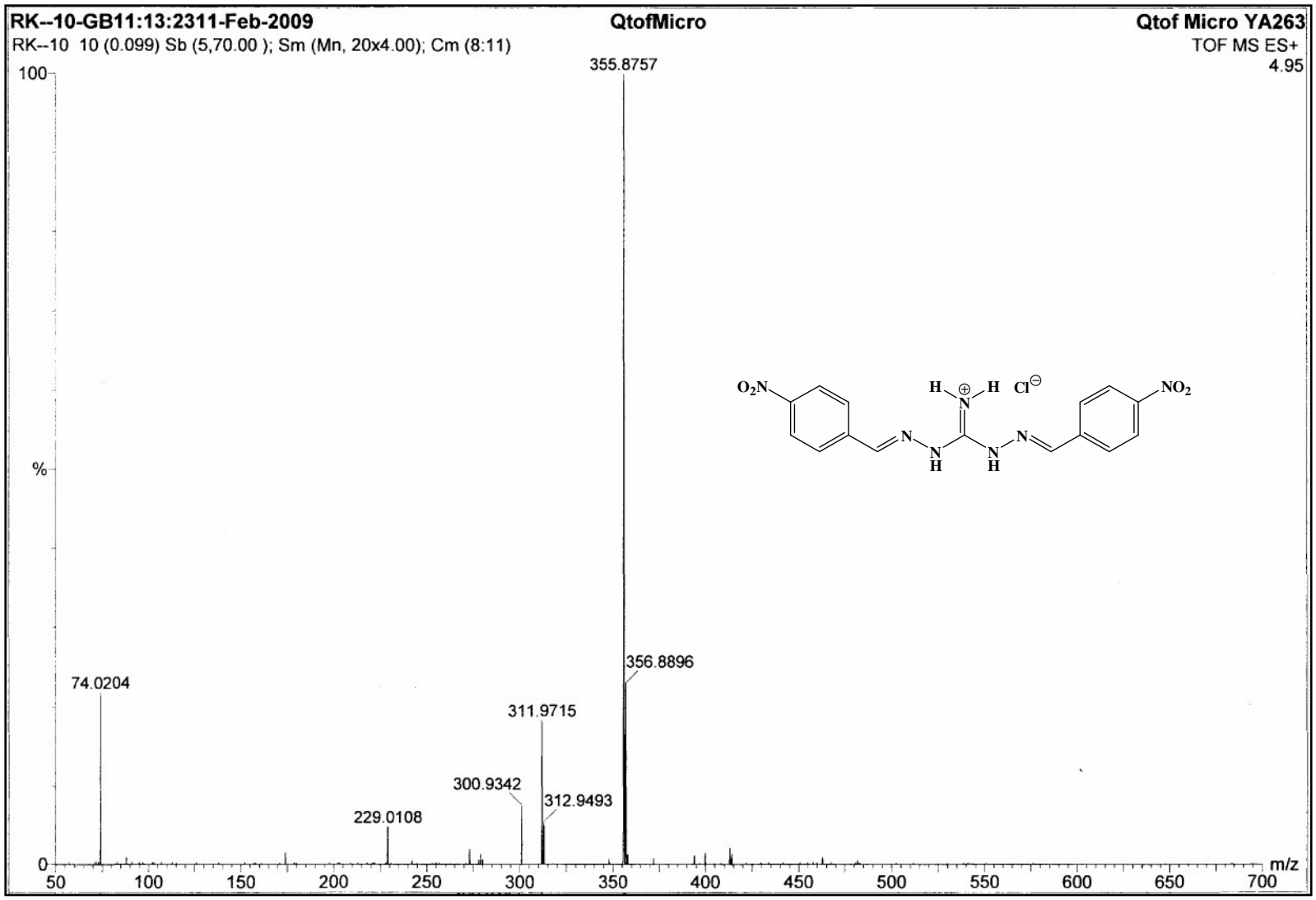

Figure S27. HRMS spectrum of **S9**.

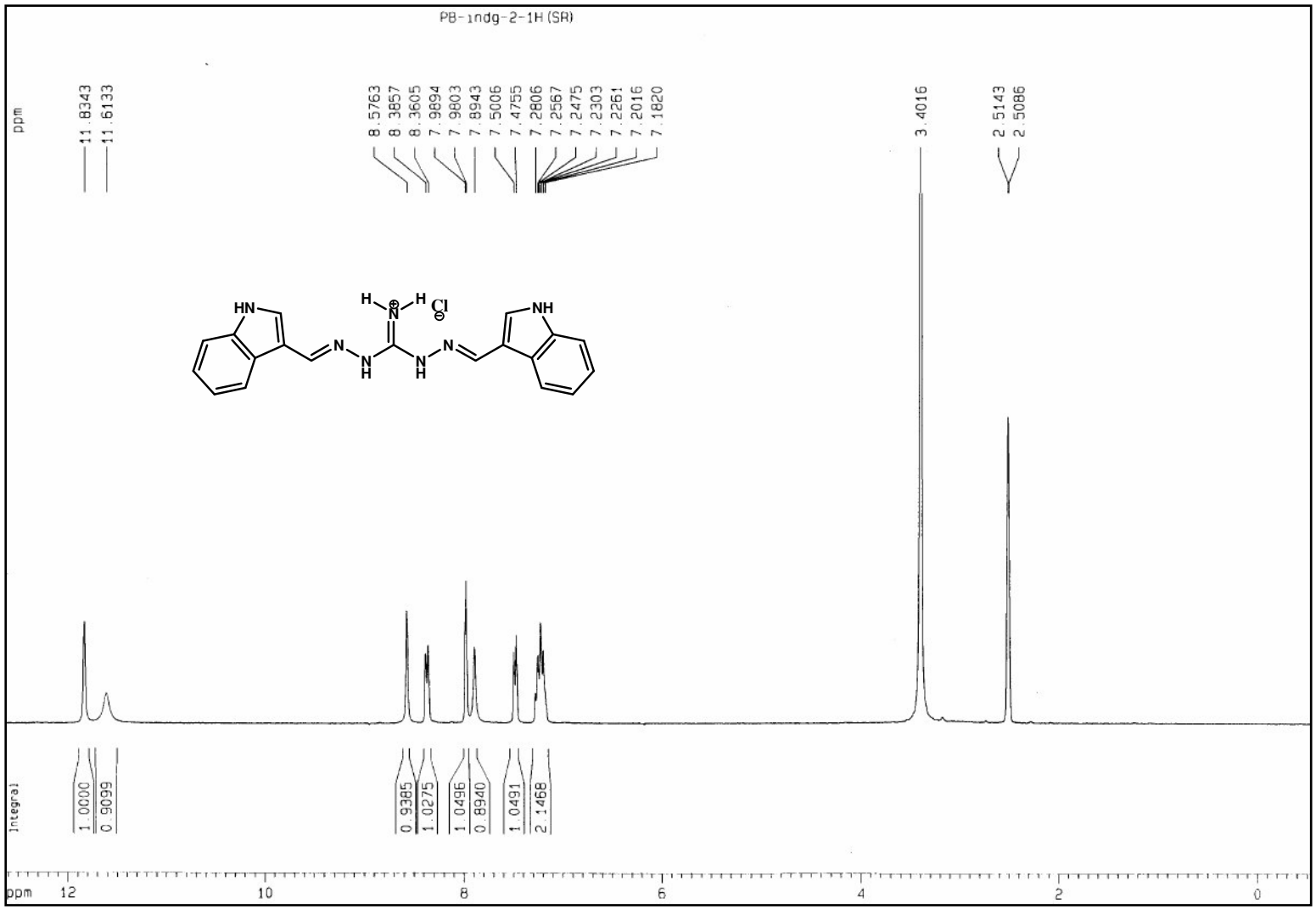

Figure S28. ^{1}H NMR spectrum of **S10** in DMSO-d_6.

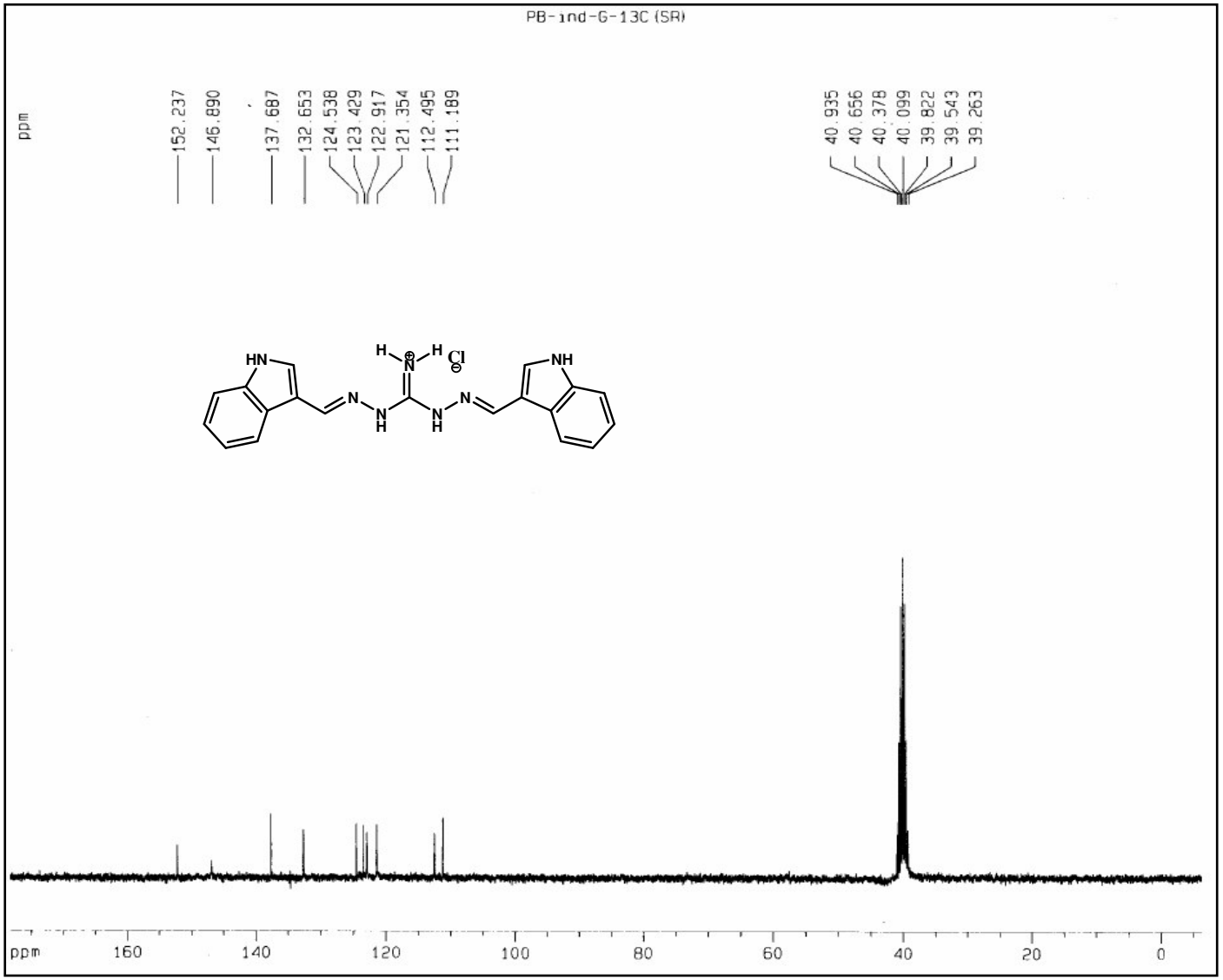

Figure S29. ^{13}C NMR spectrum of **S10** in DMSO-d_6.

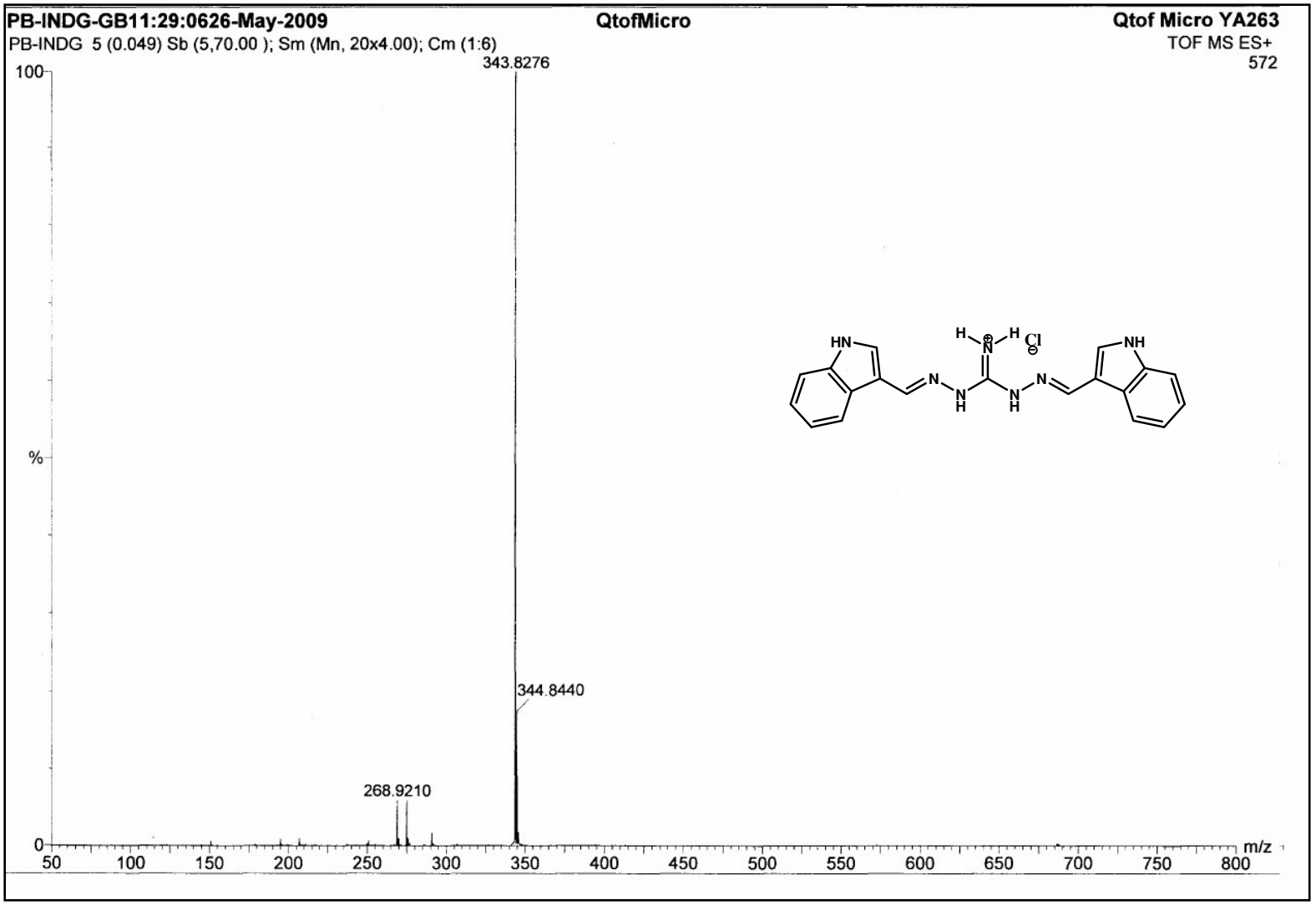

Figure S30. HRMS spectrum of **S10**.

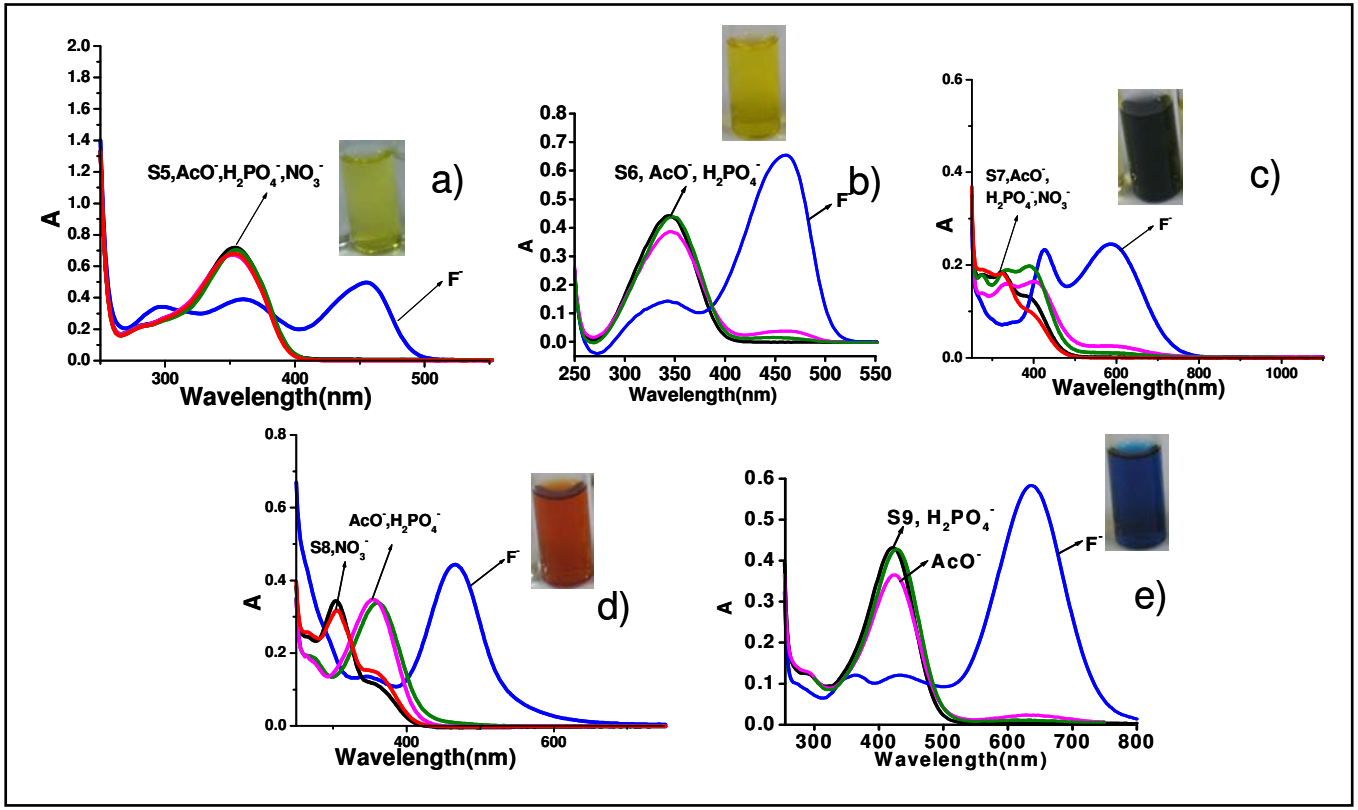

Figure S31. Changes in the UV-Vis absorption spectrum a)-e) of **S5-S9** (1.0×10^{-4} M) in MeCN/DMF (9.6:0.4)(v/v) solution upon addition of 50 equiv of anions.

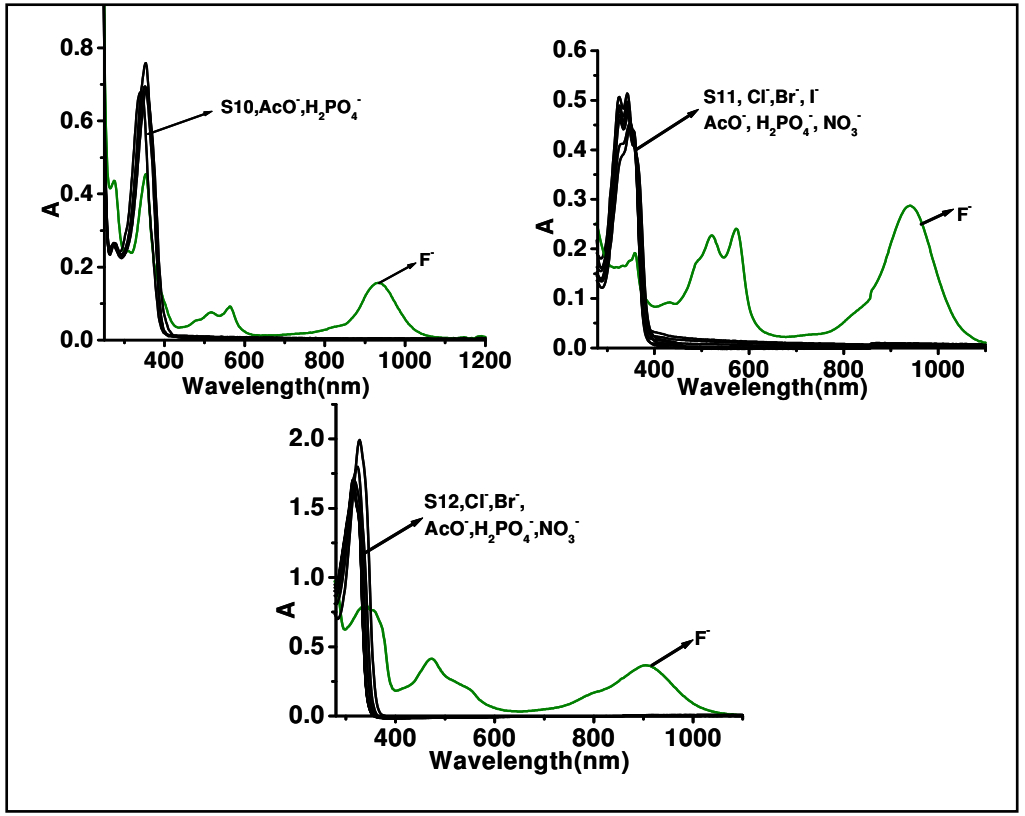

Figure S32. Changes in the UV/vis/NIR absorption spectrum of **S10-S12** (1.0×10^{-5} M) in MeCN/DMF(9.6:0.4)(v/v) solution upon addition of 50 equiv of different anions.

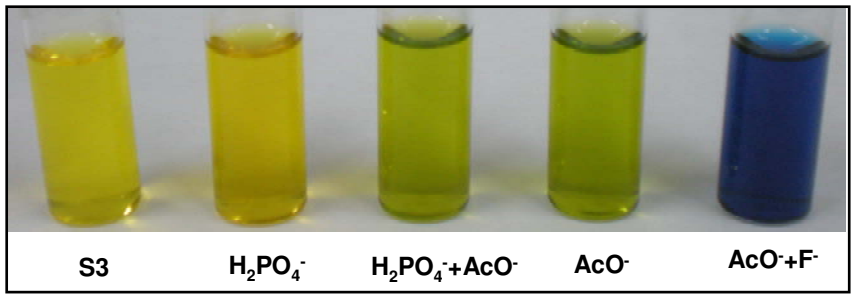

Figure S33. Selectivity study of **S9** ($1x10^{-4}$ M) in presence of different anions (30 eqiv.).

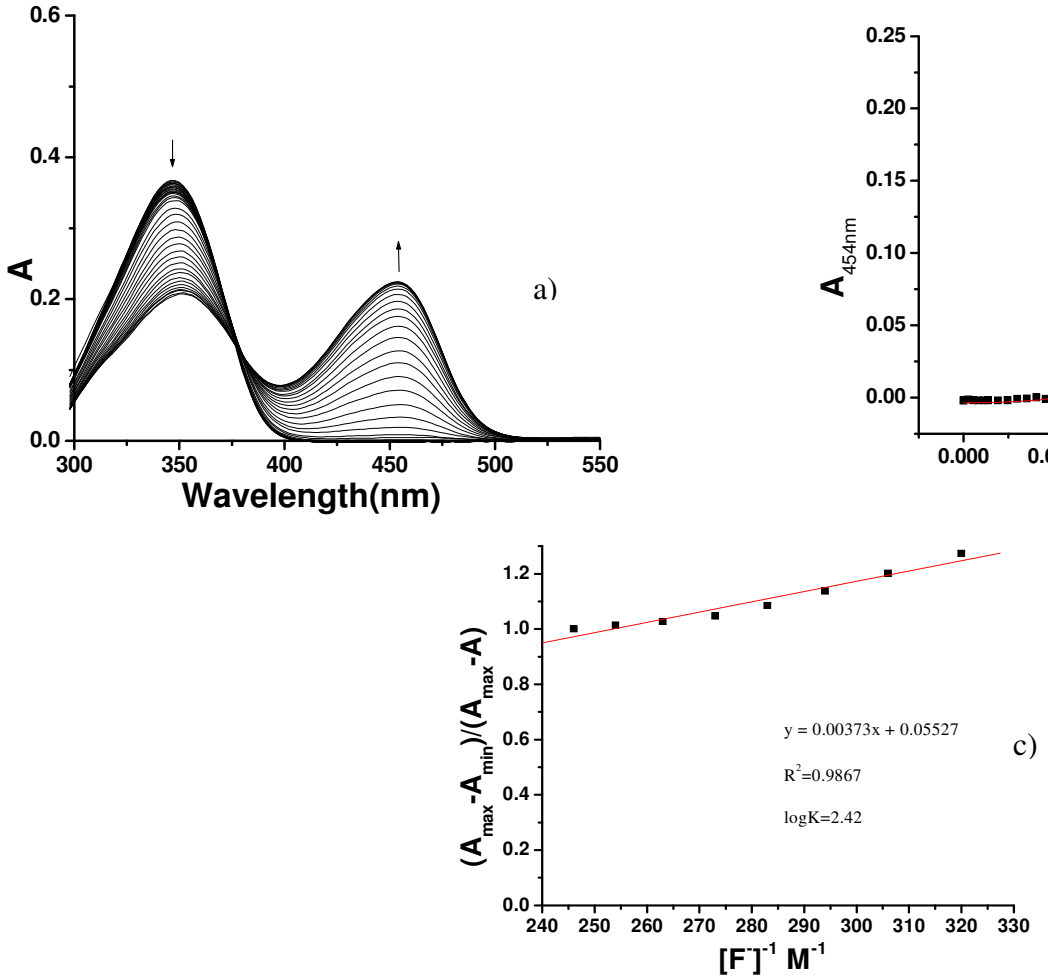

Figure S34. a) UV-Vis absorption changes of the titration of a 1.0×10^{-5} M solution of **S1** in in MeCN/DMF (9.6:0.4)(v/v) with a standard solution of 0.01 (M) $[Bu_4N]F$ in MeCN. b) Absorbance changes for **S1** at 350 nm on addition of various concentration of [Bu4N]F.c) Benesi–Hildebrand plot.

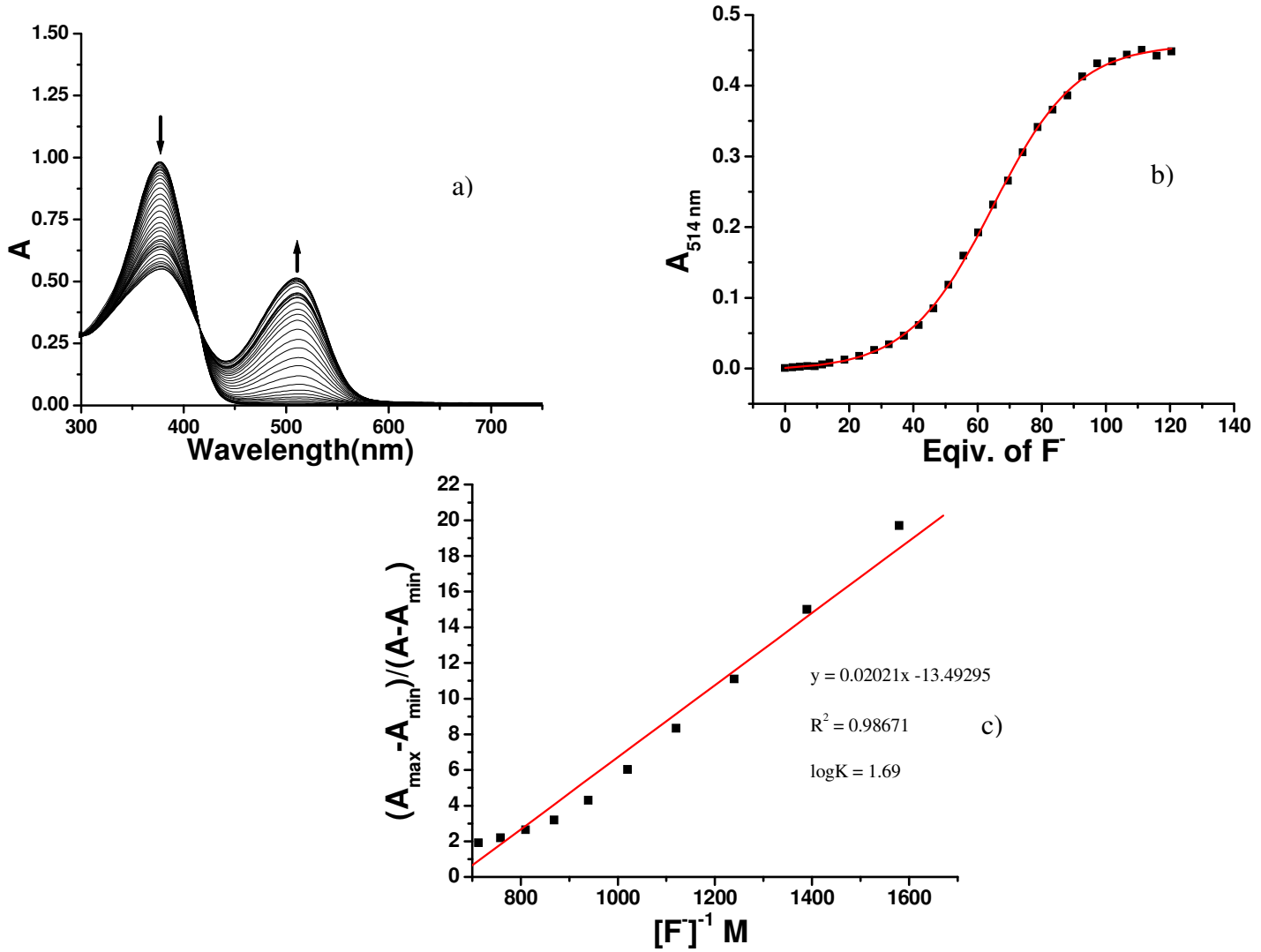

Figure S35. a) UV-Vis absorption changes of the titration of a 1.0×10^{-5} M solution of **S2** in in MeCN/DMF(9.6:0.4)(v/v) with a standard solution of 0.01(M) $[Bu_4N]F$ in MeCN. b) Absorbance changes for S**2** at 514 nm on addition of various concentration of $[Bu_4N]F$. c) Benesi–Hildebrand plot.

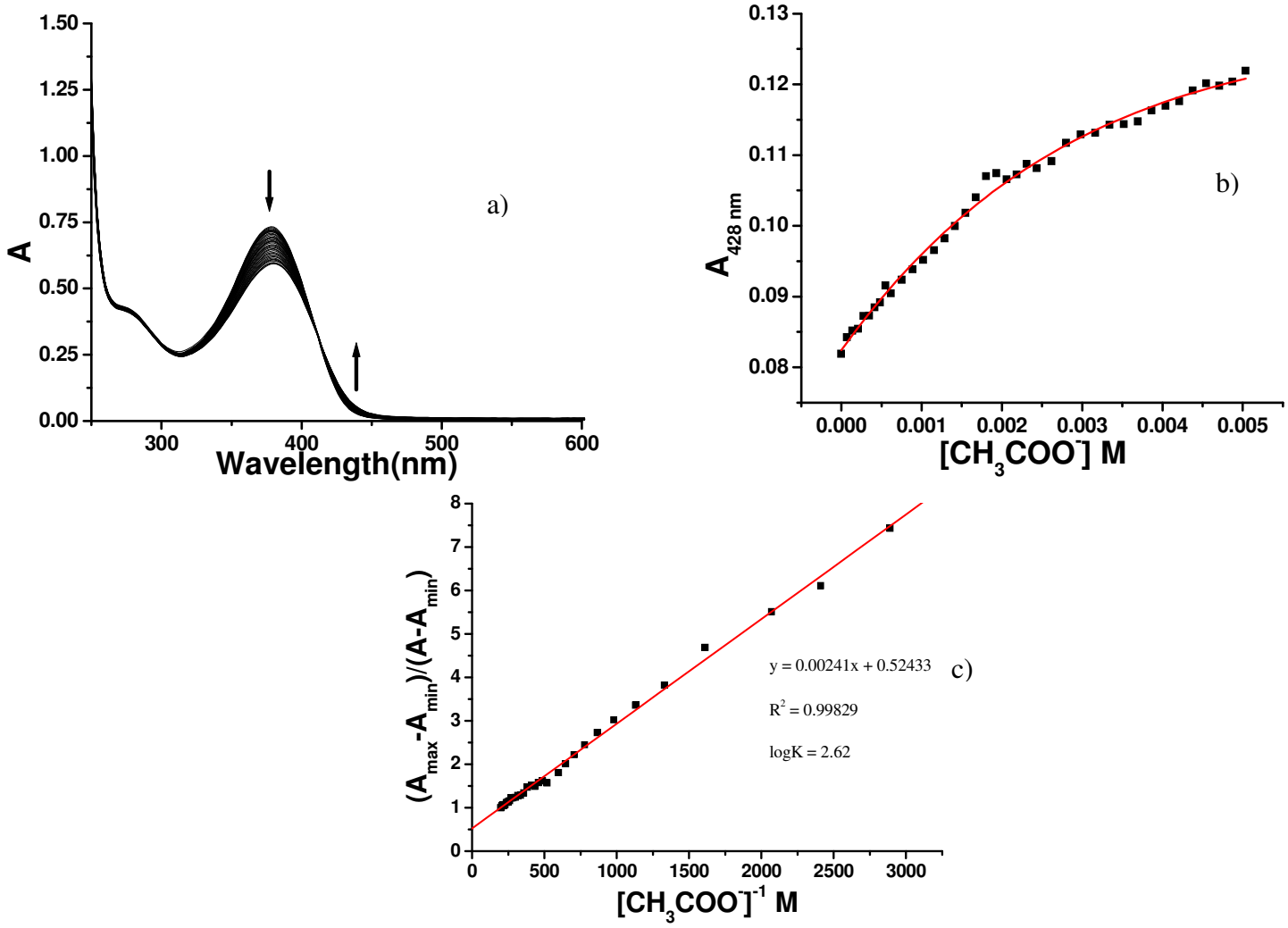

Figure S36. a) UV-Vis absorption changes of the titration of a 1.0×10^{-5} M solution of **S2** in in MeCN/DMF(9.6:0.4)(v/v) with a standard solution of 0.01(M) $[Bu_4N]AcO$ in MeCN. b) Absorbance changes for **S2** at 428 nm on addition of various concentration of $[Bu_4N]AcO$.c) Benesi–Hildebrand plot.

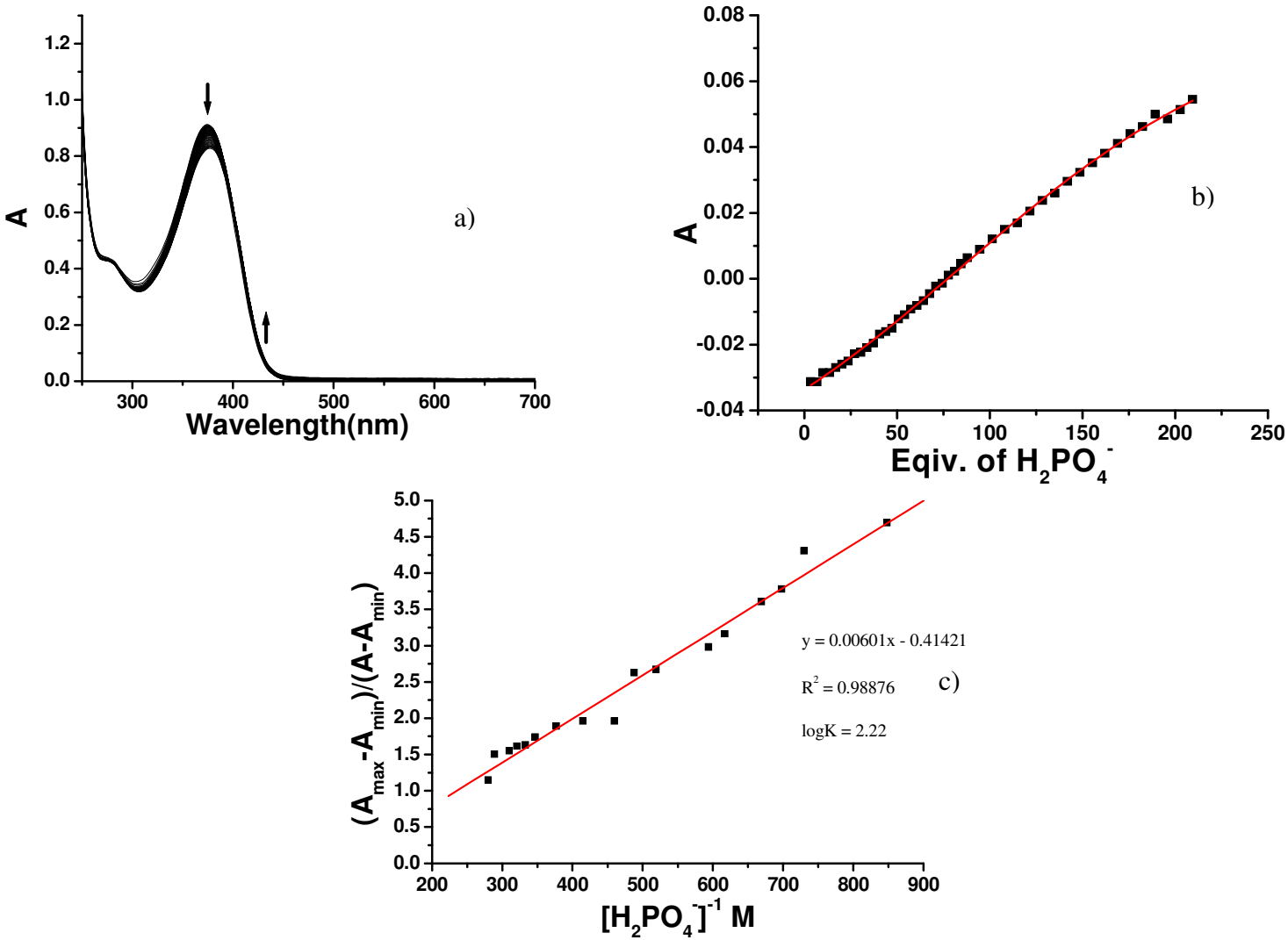

Figure S37. a) UV-Vis absorption changes of the titration of a 1.0×10^{-5} M solution of **S2** in in MeCN/DMF (9.6:0.4)(v/v) with a standard solution of 0.01(M) $[Bu_4N]H_2PO_4$ in MeCN. b) Absorbance changes for **S2** at 430 nm on addition of various concentration of $[Bu_4N]$ H_2PO_4. c) Benesi–Hildebrand plot.

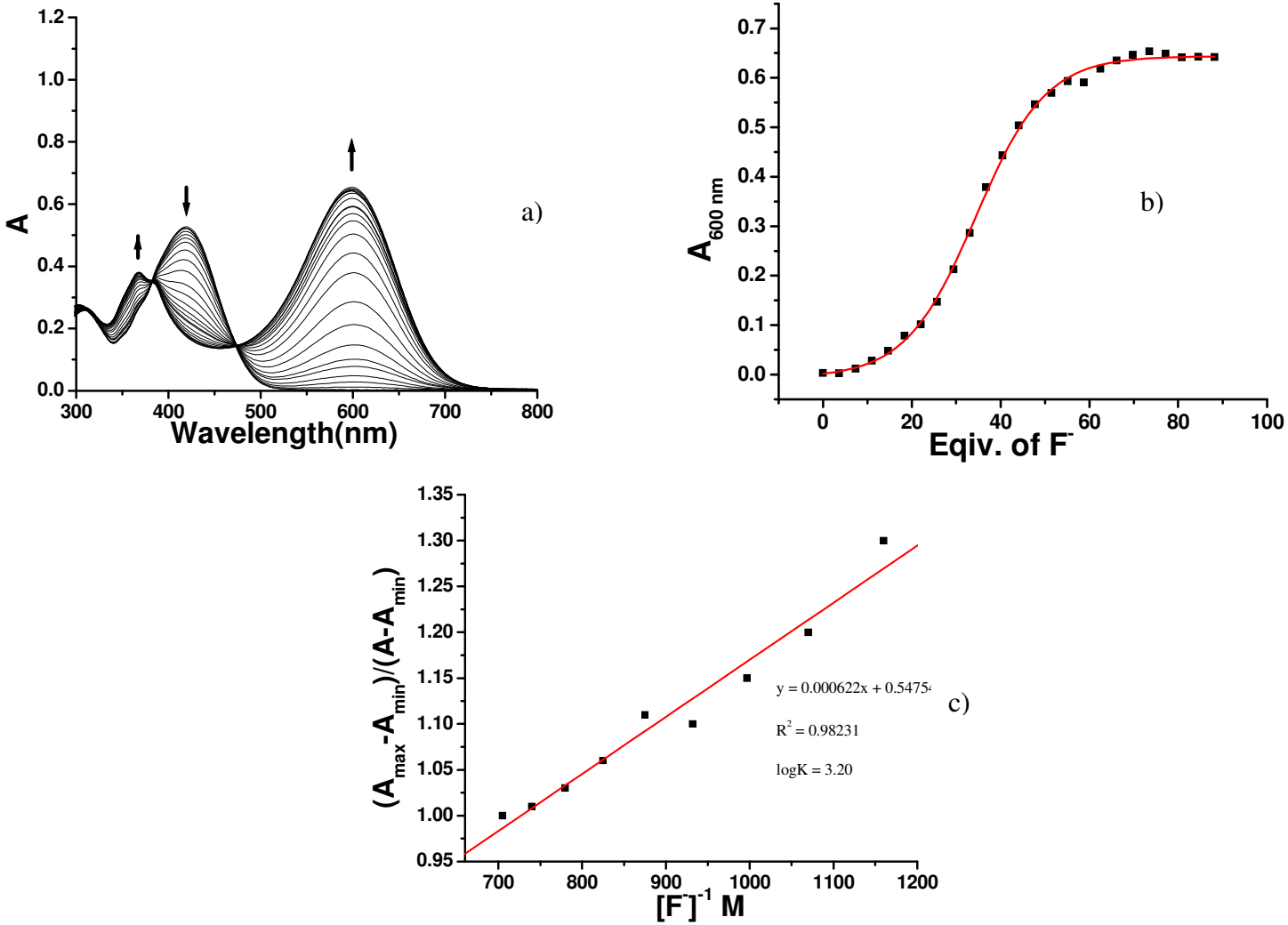

Figure S38. a) UV-Vis absorption changes of the titration of a 1.0×10^{-5} M solution of **S3** in in MeCN/DMF(9.6:0.4)(v/v) with a standard solution of 0.01(M) $[Bu_4N]F$ in MeCN. b) Absorbance changes for **S3** at 600 nm on addition of various concentration of $[Bu_4N]F$.c) Benesi–Hildebrand plot.

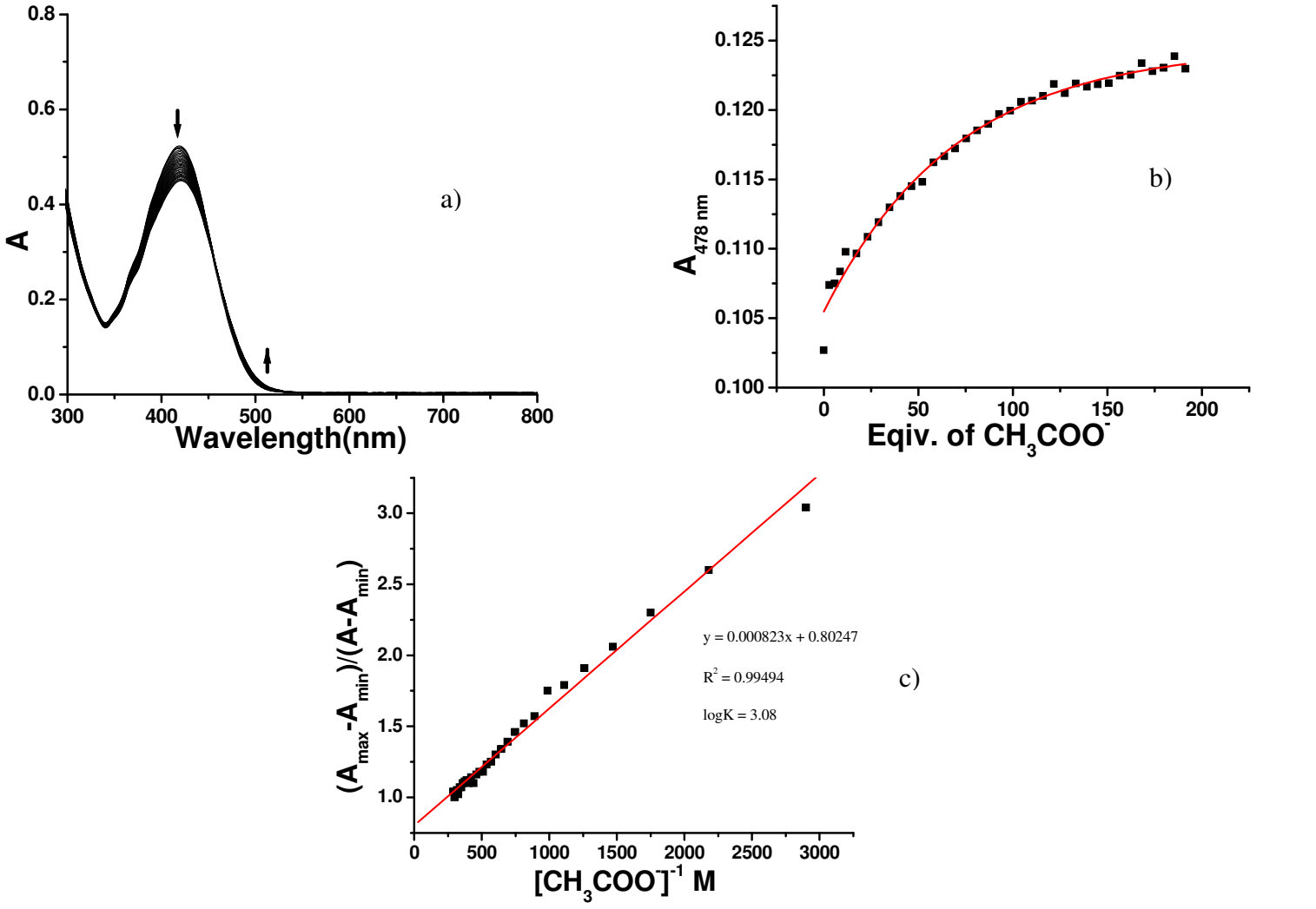

Figure S39. a) UV-Vis absorption changes of the titration of a 1.0×10^{-5} M solution of **S3** in in MeCN/DMF (9.6:0.4)(v/v) with a standard solution of 0.01(M) $[Bu_4N]AcO$ in MeCN. b) Absorbance changes for **S3** at 478 nm on addition of various concentration of $[Bu_4N]AcO$. c) Benesi–Hildebrand plot.

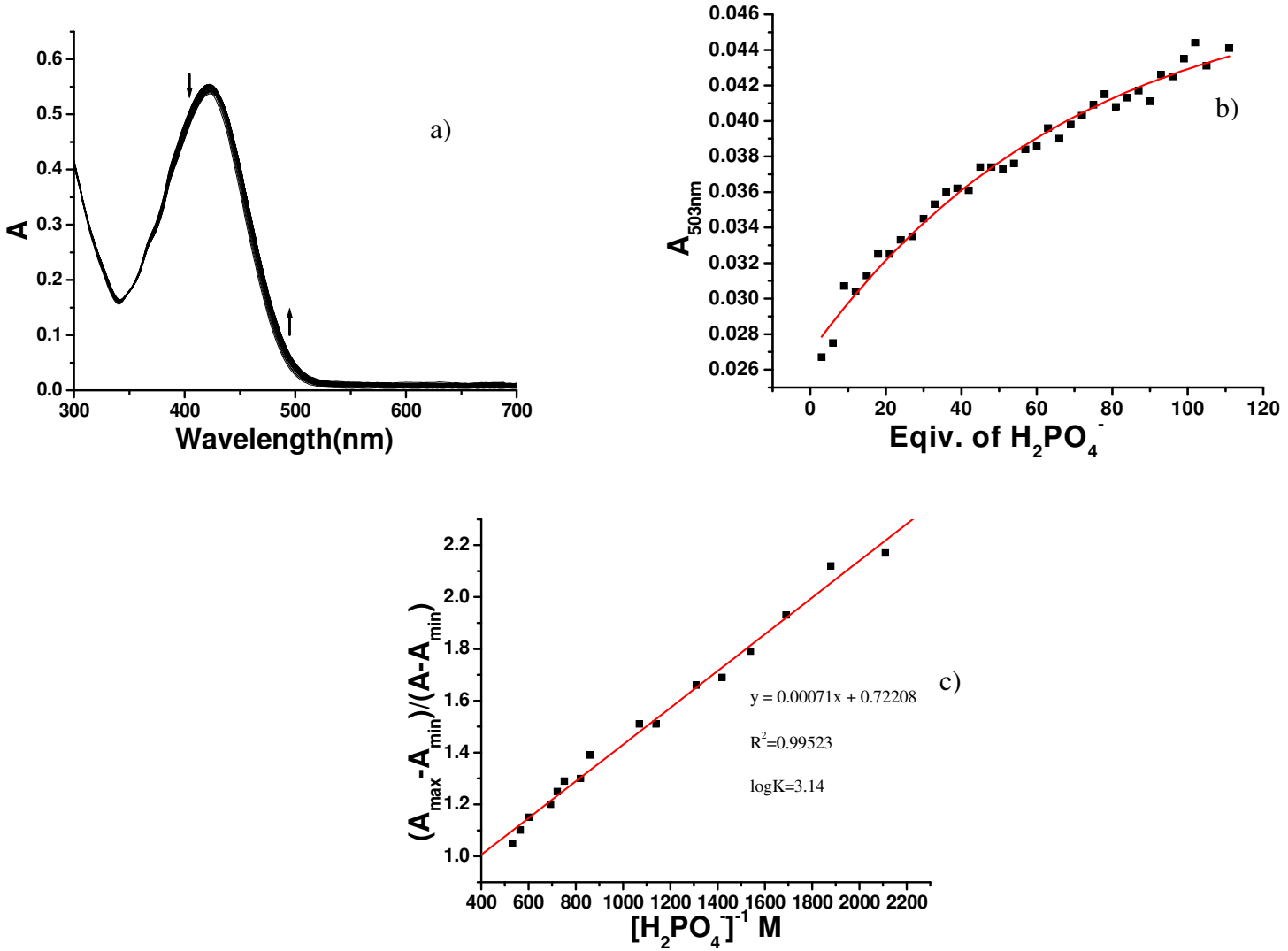

Figure S40. a) UV-Vis absorption changes of the titration of a 1.0×10^{-5} M solution of **S3** in in MeCN/DMF(9.6:0.4)(v/v) with a standard solution of 0.01(M) $[Bu_4N]H_2PO_4$ in MeCN. b) Absorbance changes for **S3** at 503 nm on addition of various concentration of $[Bu_4N]H_2PO_4$.c) Benesi–Hildebrand plot.

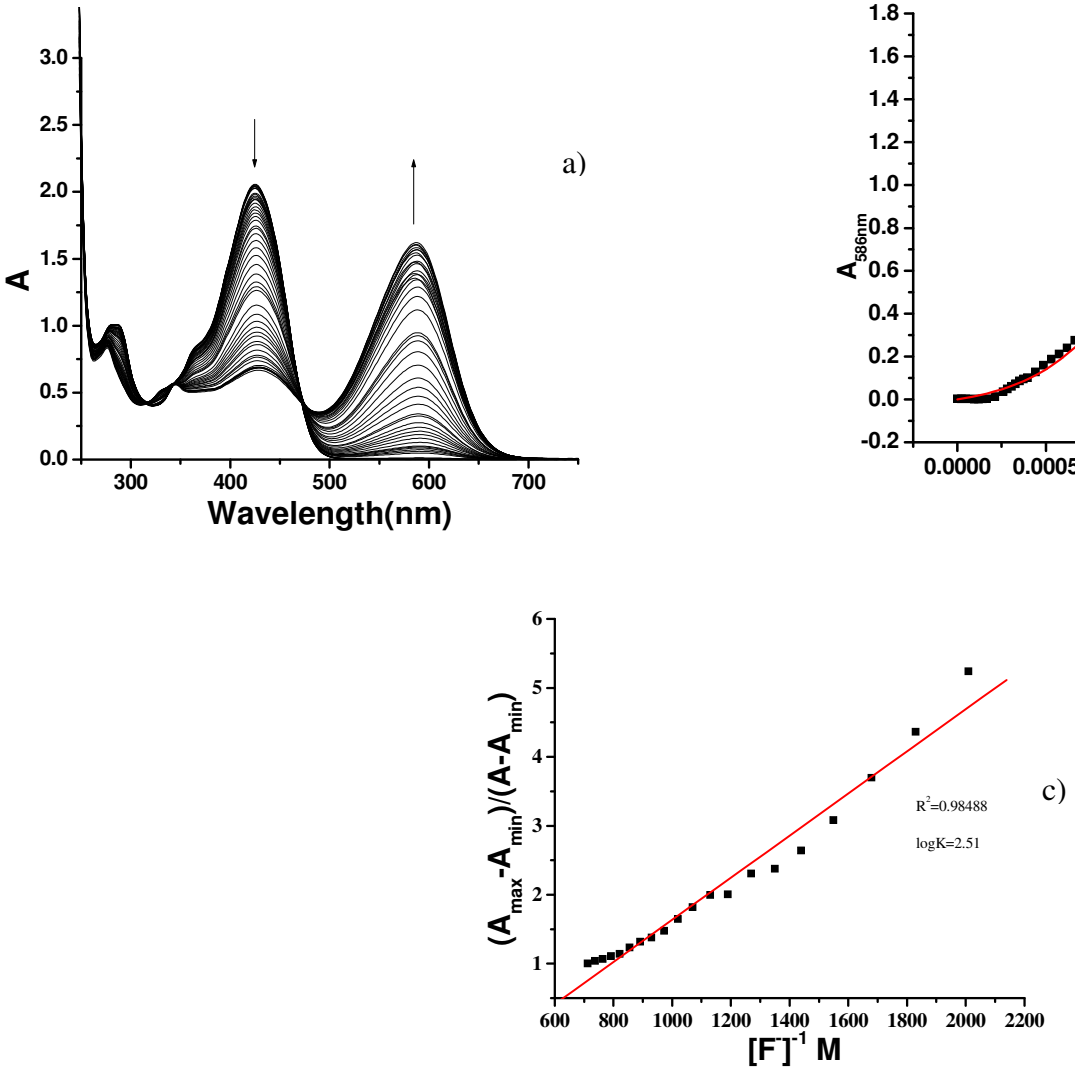

Figure S41. a) UV-Vis absorption changes of the titration of a 1.0×10^{-5} M solution of **S4** in in MeCN/DMF(9.6:0.4)(v/v) with a standard solution of 0.01 (M) $[Bu_4N]F$ in MeCN. b) Absorbance changes for **S4** at 586 nm on addition of various concentration of $[Bu_4N]F$.c) Benesi–Hildebrand plot.

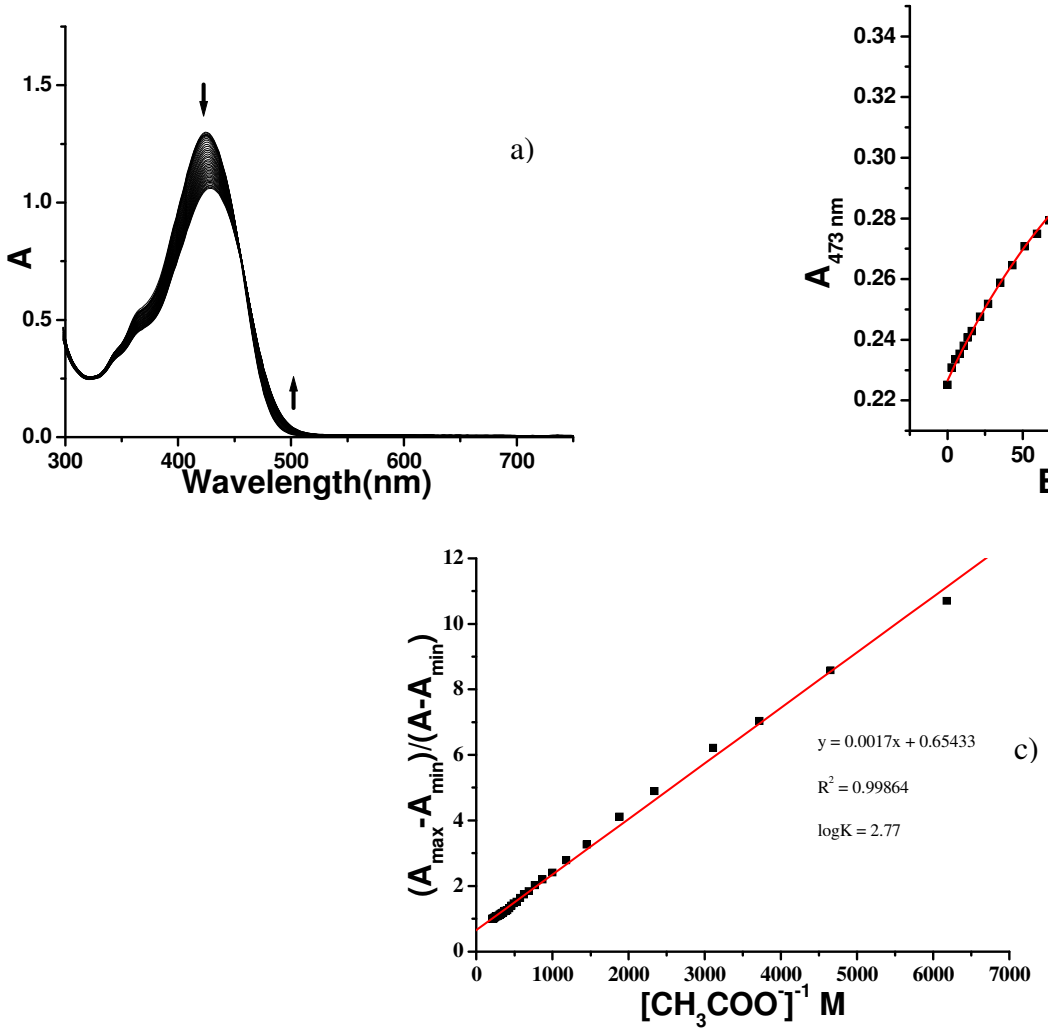

Figure S42. a) UV-Vis absorption changes of the titration of a 1.0×10^{-5} M solution of **S4** in in MeCN/DMF (9.6:0.4)(v/v) with a standard solution of 0.01 (M) $[Bu_4N]AcO$ in MeCN. b) Absorbance changes for **S4** at 473 nm on addition of various concentration of $[Bu_4N]AcO$.c) Benesi–Hildebrand plot.

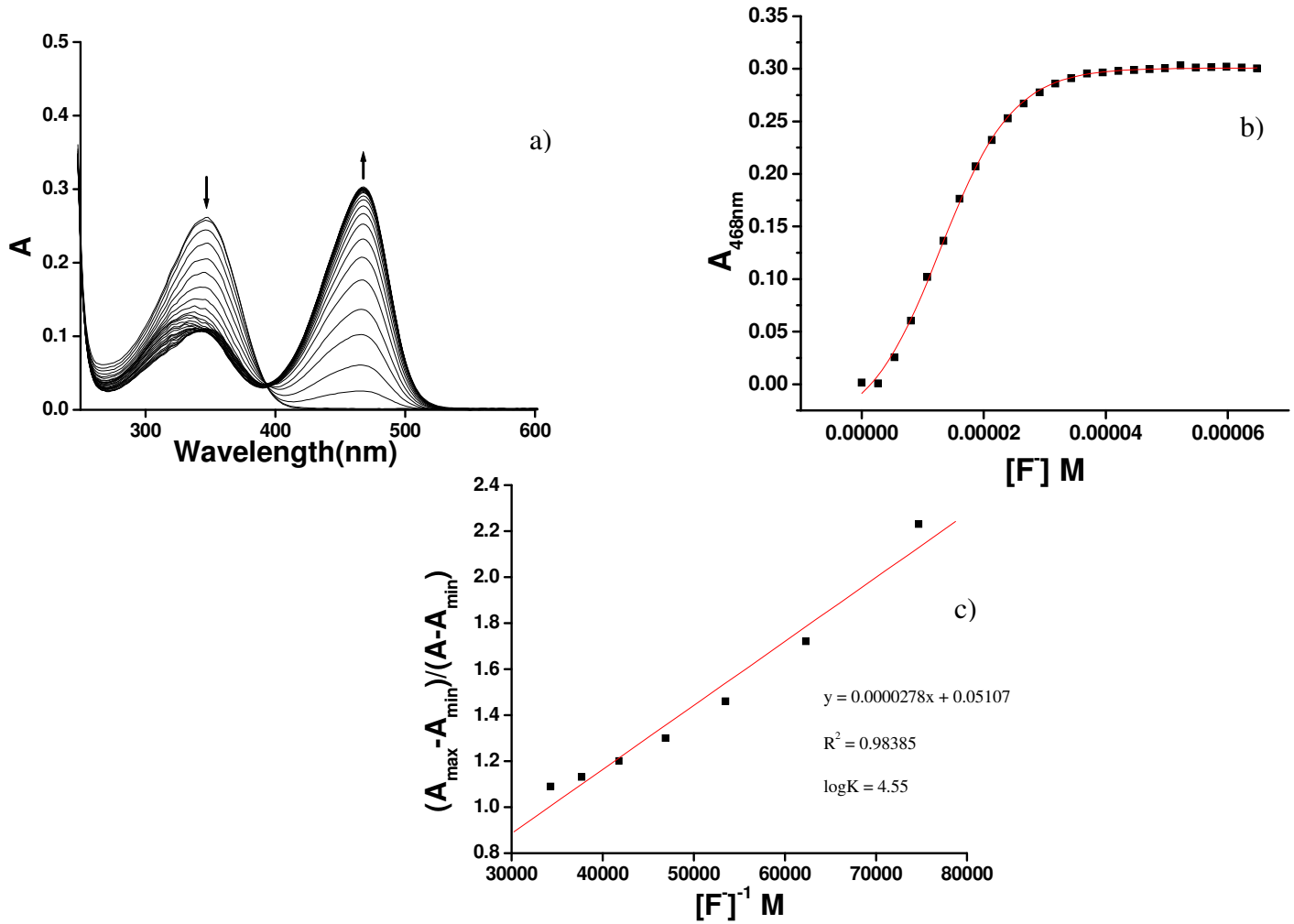

Figure S43. a) UV-Vis absorption changes of the titration of a 1.0×10^{-5} M solution of **S6** in in MeCN/DMF (9.6:0.4)(v/v) with a standard solution of 0.01 (M) $[Bu_4N]F$ in MeCN. b) Absorbance changes for **S6** at 468 nm on addition of various concentration of $[Bu_4N]F$. c) Benesi–Hildebrand plot.

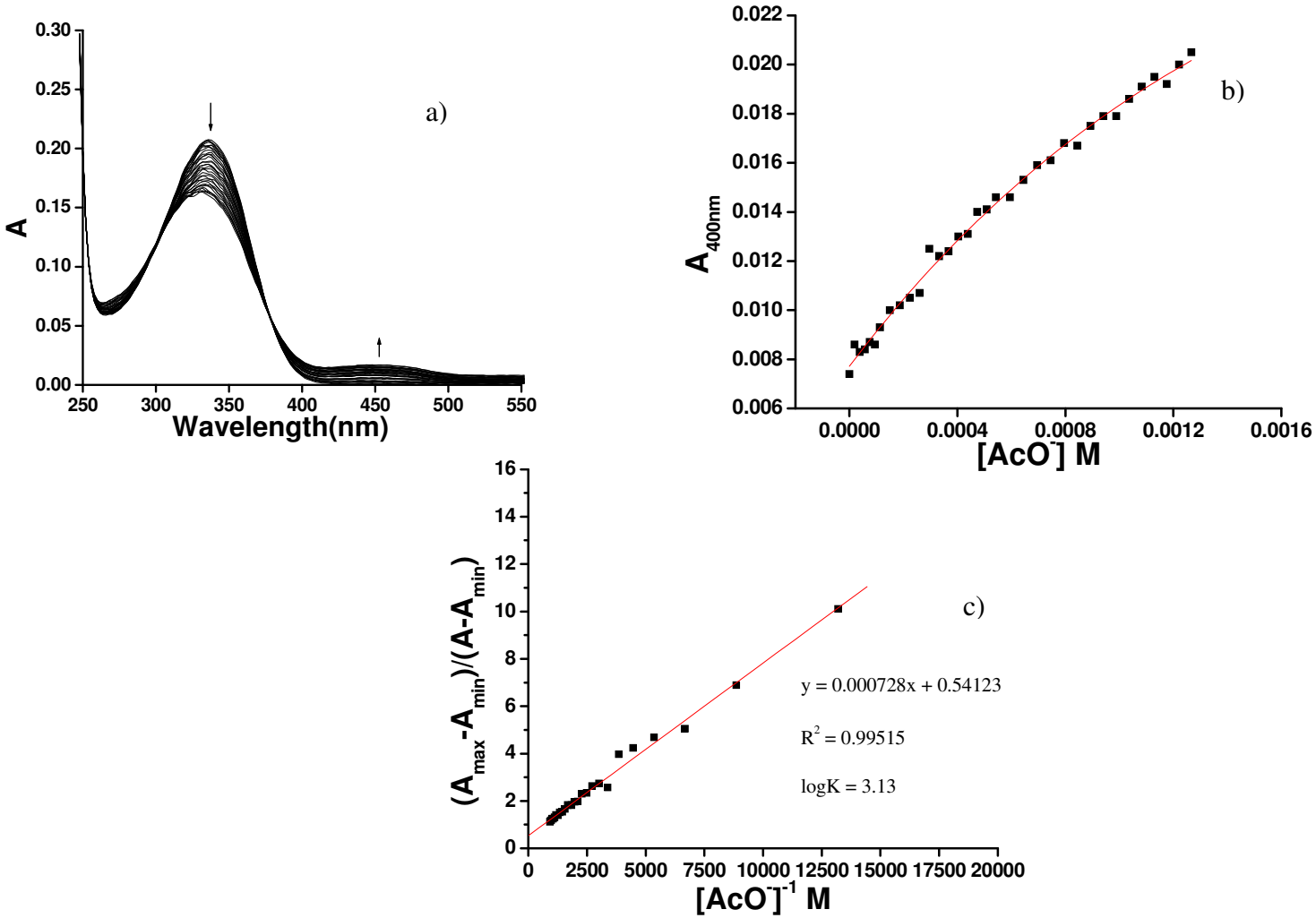

Figure S44. a) UV-Vis absorption changes of the titration of a 1.0×10^{-5} M solution of **S6** in in MeCN/DMF(9.6:0.4)(v/v) with a standard solution of 0.01(M) $[Bu_4N]AcO$ in MeCN. b) Absorbance changes for **S6** at 468 nm on addition of various concentration of $[Bu_4N]AcO$.c) Benesi–Hildebrand plot.

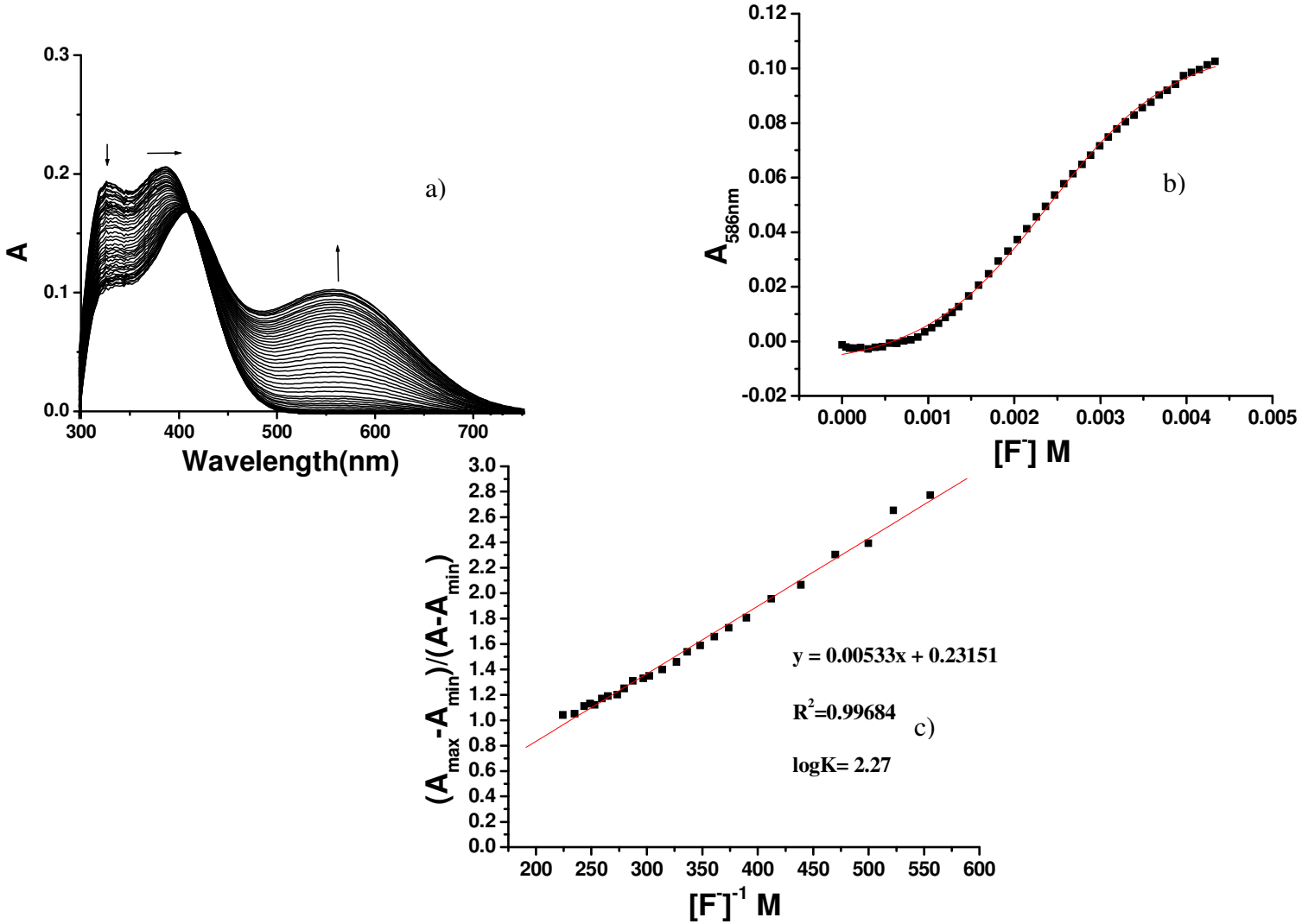

Figure S45. a) UV-Vis absorption changes of the titration of a 1.0×10^{-5} M solution of **S7** in in MeCN/DMF(9.6:0.4)(v/v) with a standard solution of 0.01 (M) $[Bu_4N]F$ in MeCN. b) Absorbance changes for **S7** at 586 nm on addition of various concentration of $[Bu_4N]F$.c) Benesi–Hildebrand plot.

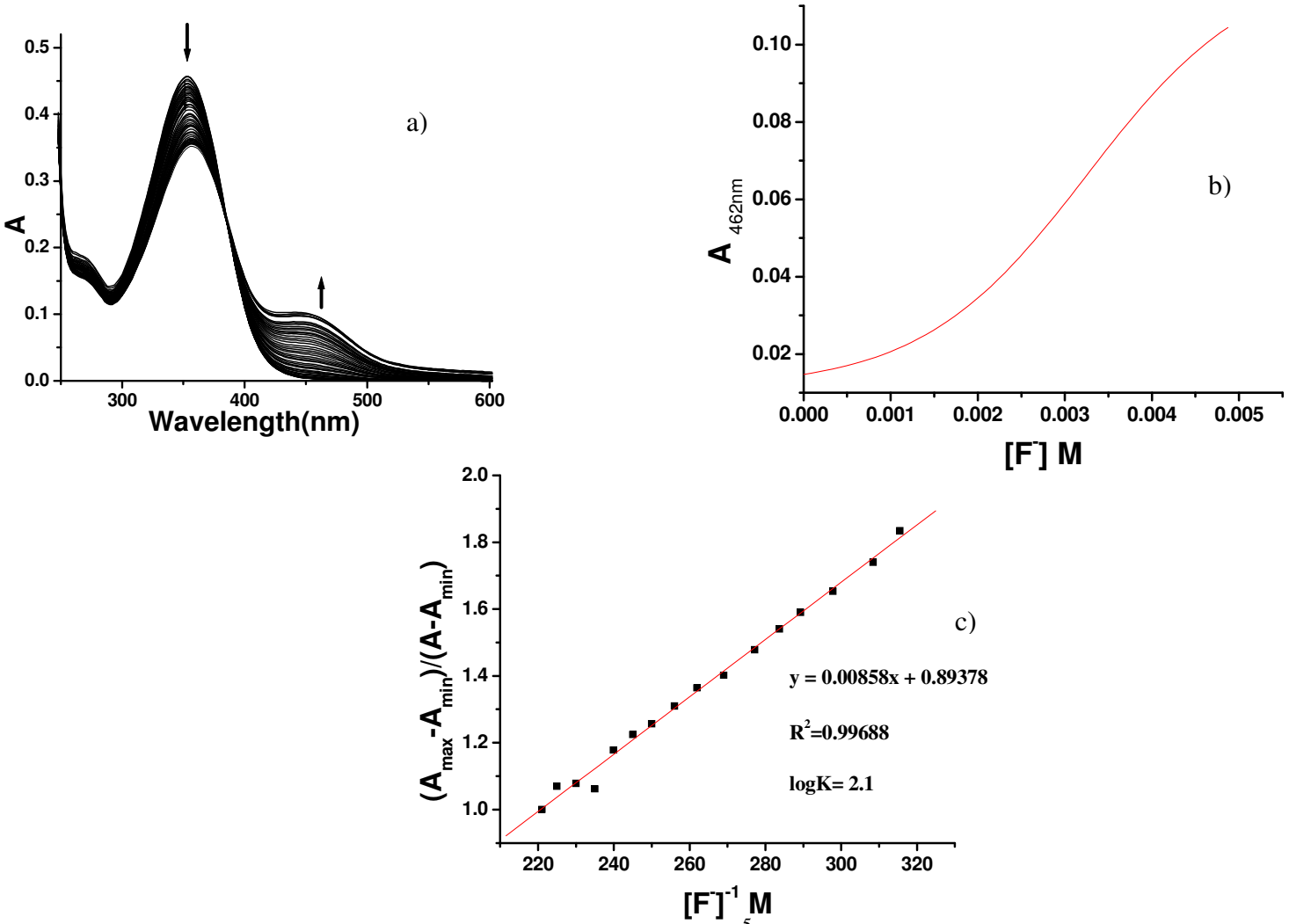

Figure S46. a) UV-Vis absorption changes of the titration of a 1.0×10^{-5} M solution of **S8** in in MeCN/DMF (9.6:0.4)(v/v) with a standard solution of 0.01 (M) $[Bu_4N]F$ in MeCN. b) Absorbance changes for **S8** at 462 nm on addition of various concentration of $[Bu_4N]F$. c) Benesi–Hildebrand plot.

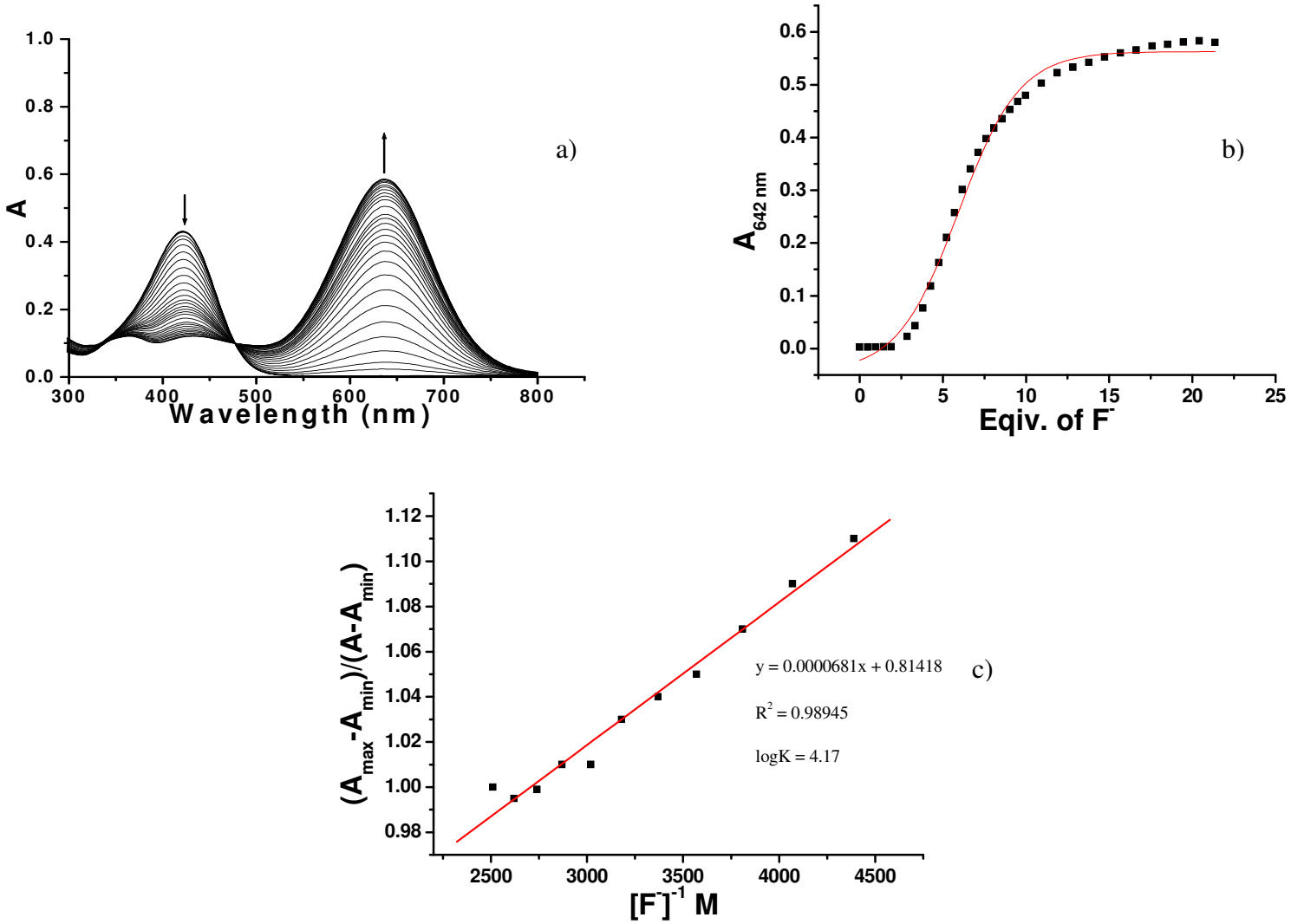

Figure S47. a) UV-Vis absorption changes of the titration of a 1.0×10^{-5} M solution of **S9** in in MeCN/DMF(9.6:0.4)(v/v) with a standard solution of 0.01 (M) $[Bu_4N]F$ in MeCN. b) Absorbance changes for **S9** at 642 nm on addition of various concentration of $[Bu_4N]F$.c) Benesi–Hildebrand plot.

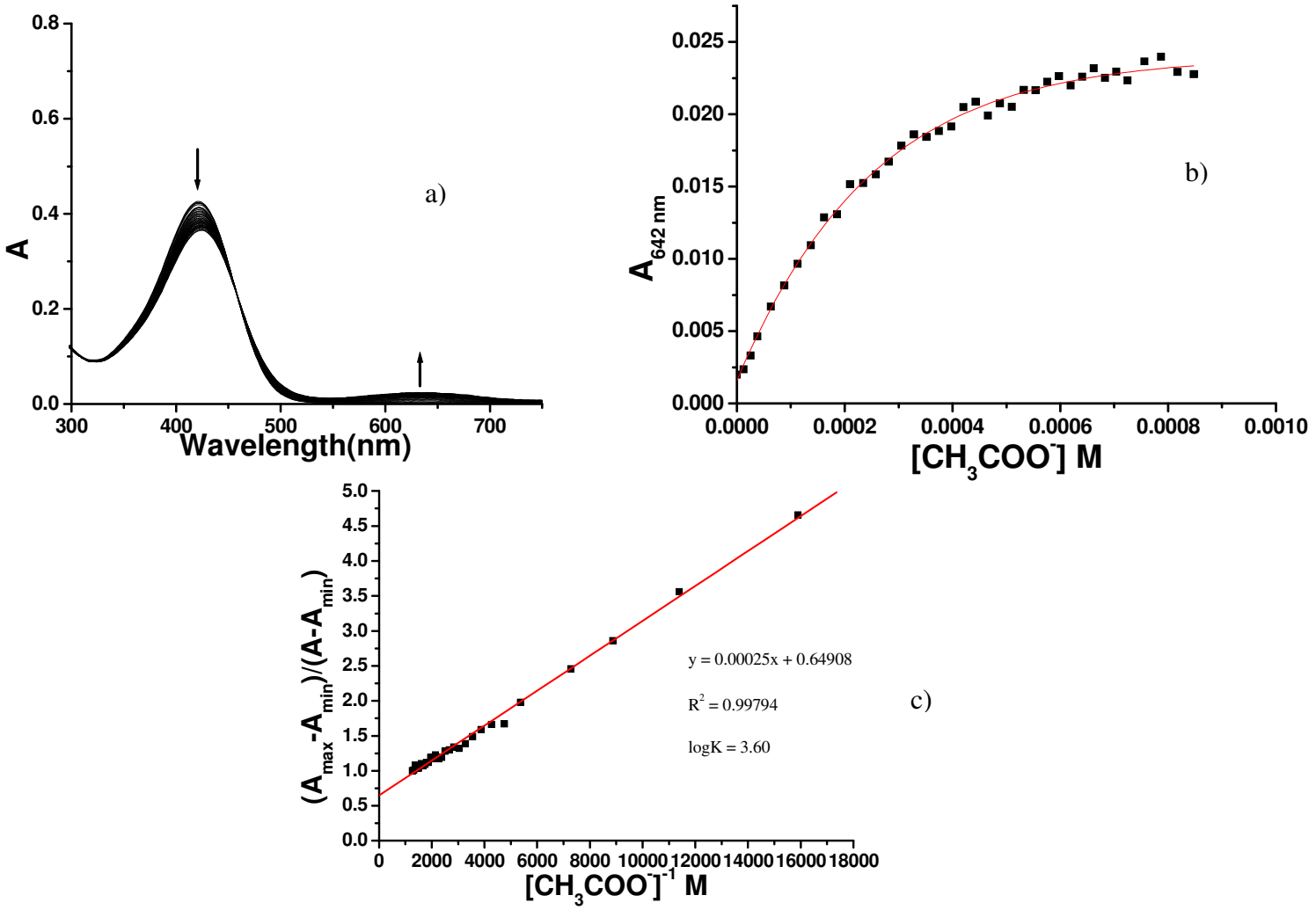

Figure S48. a) UV-Vis absorption changes of the titration of a 1.0×10^{-5} M solution of **S9** in in MeCN/DMF(9.6:0.4)(v/v) with a standard solution of 0.01 (M) $[Bu_4N]AcO$ in MeCN. b) Absorbance changes for **S9** at 642 nm on addition of various concentration of $[Bu_4N]AcO$.c) Benesi–Hildebrand plot.

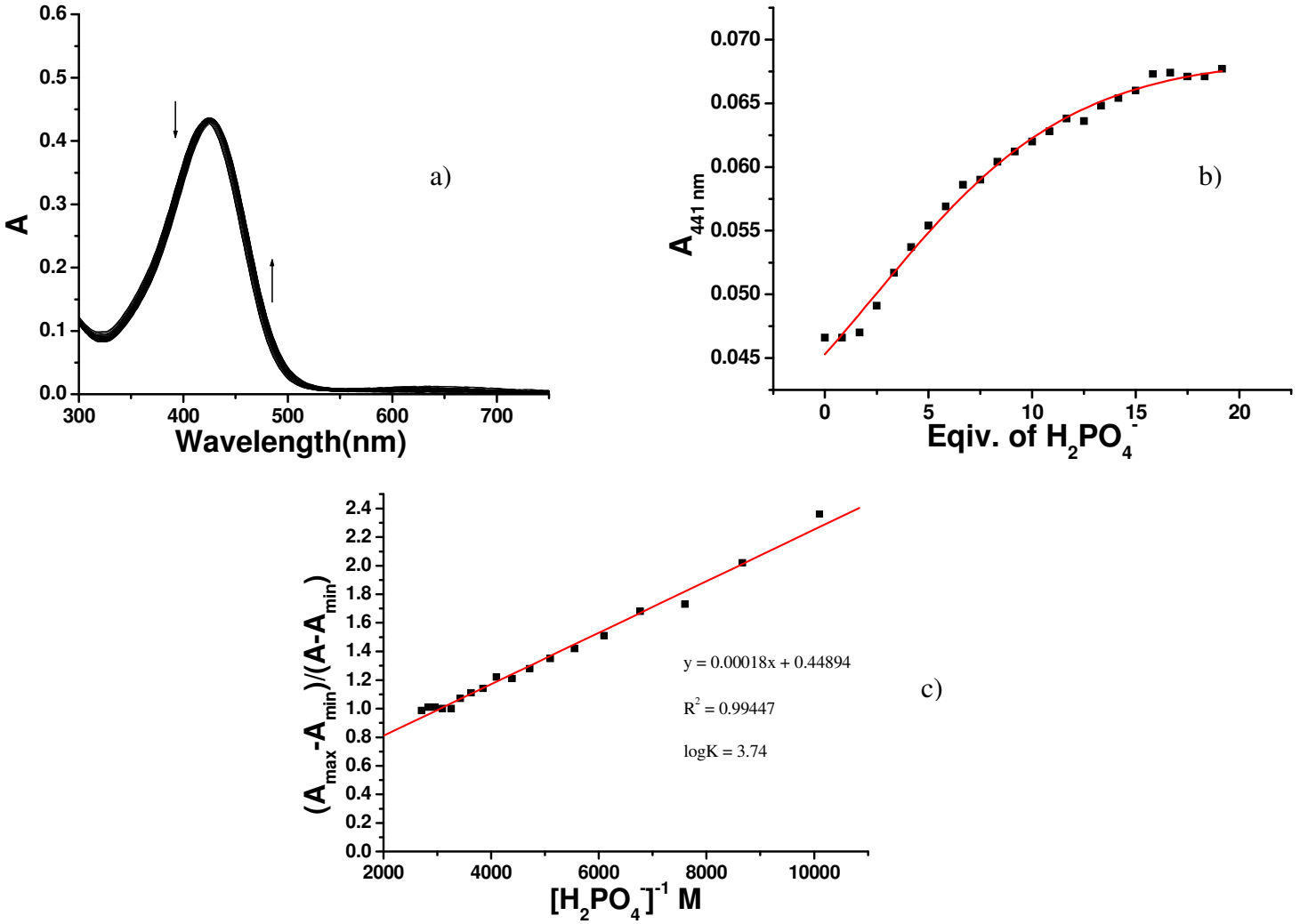

Figure S49. a) UV-Vis absorption changes of the titration of a 1.0×10^{-5} M solution of **S9** in in MeCN/DMF(9.6:0.4)(v/v) with a standard solution of 0.01 (M) $[Bu_4N]H_2PO_4$ in MeCN. b) Absorbance changes for **S9** at 441 nm on addition of various concentration of $[Bu_4N]H_2PO_4$.c) Benesi–Hildebrand plot.

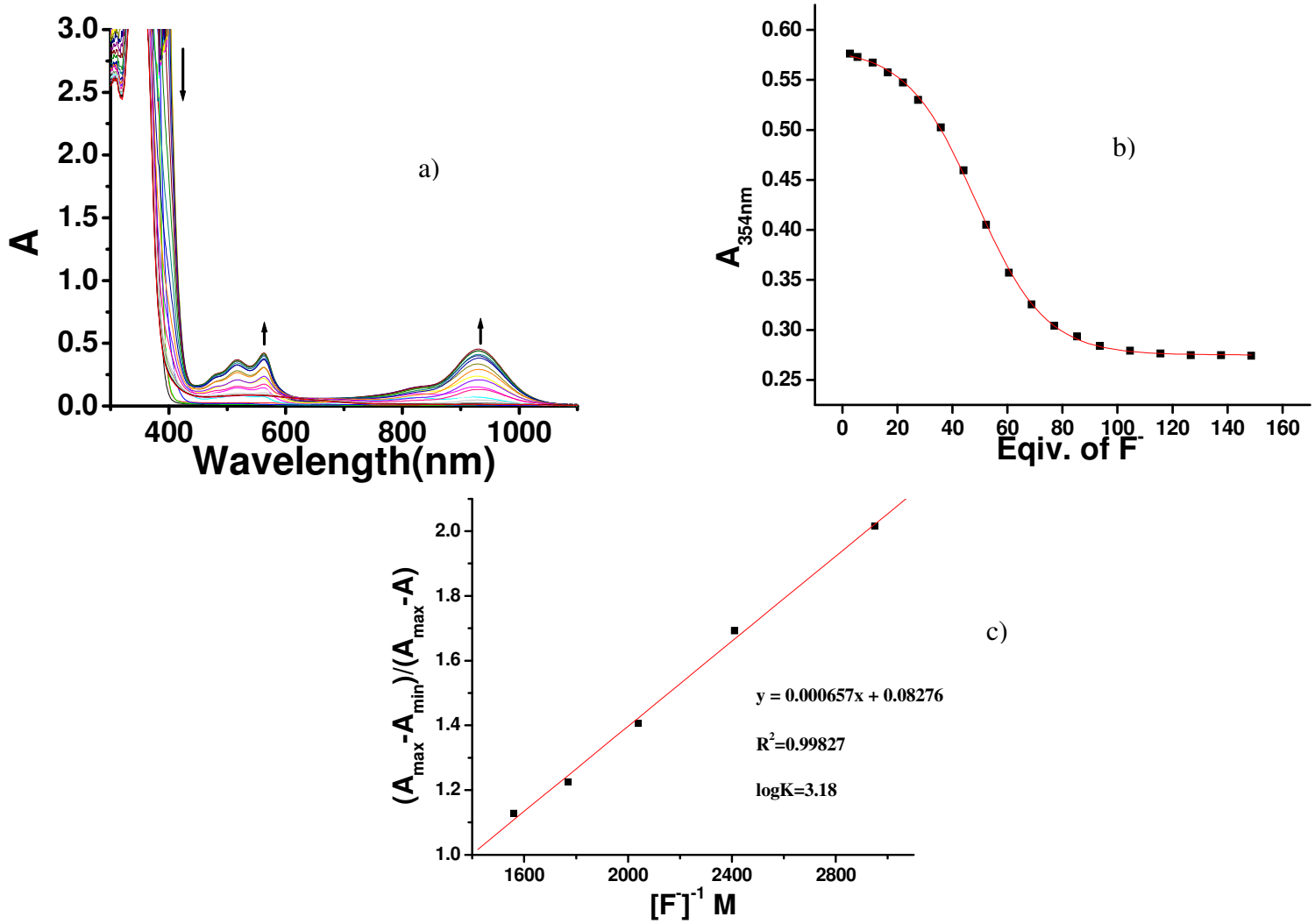

Figure S50. a) UV-Vis absorption changes of the titration of a 1.0×10^{-5} M solution of **S10** in in MeCN/DMF(9.6:0.4)(v/v) with a standard solution of 0.01(M) $[Bu_4N]F$ in MeCN. b) Absorbance changes for **S10** at 354 nm on addition of various concentration of $[Bu_4N]F$.c) Benesi–Hildebrand plot.

Table S1. Table of Crystallographic parameters

Parameters	**1**	**Complex 2**	**Complex 3**
Empirical formula	C_{16} H_9 F_{10} N_5 O	C_{36} H_{22} F_{10} N_5 O_6	$C_{37}H_{31}$ N_5 O_4
Formula weight	477.28	810.59	609.67
crystal system	Monoclinic	Monoclinic	Orthorhombic
Space group	P2(1)/n	P2(1)/m	Pbca
***a* (Å)**	16.012(10)	6.8654(13)	14.5032(10)
***b* (Å)**	11.932(7)	34.567(6)	9.6882(7)
***c* (Å)**	19.682(12)	7.1380(14)	44.522(3)
α (deg)	90.00	90.000	90.000
β (deg)	104.571(8)	98.565(4)	90.000
γ (deg)	90.00	90.000	90.000
***V* (Å^3)**	3639(4)	1675.1(5)	6255.7 (8)
Z	8	2	8
d_{calc} (g/cm^3)	1.742	1.607	1.295
Crystal size (mm^3)	0.32 x 0.07 x 0.05	0.15 x 0.09 x 0.08	0.18 x 0.03x 0.02
Diffractometer	Smart CCD	Smart CCD	Smart CCD
***F*(000)**	1904	822	2560
μ MoKα (mm^{-1})	0.184	0.148	0.086
***T* (K)**	120 (2)	100 (2)	100(2)
θ max	24.39	25.00	25.00
ObservedReflections	23147	15838	55819
Parameters refined	633	232	417
R_1; WR_2	0.0499 ; 0.1123	0.0334 ; 0.0842	0.0879 ; 0.2308
GOF (F2)	1.022	1.078	1.161

Table S2. Hydrogen bonding interactions in 1.

D-H•••A	D-H (Å)	H•••A(Å)	D•••A(Å)	∟D-H•••A
N9-H9···O42	0.843	1.944	2.766(5)	165.0
O44-H44···N12	0.800	2.042	2.807(6)	160.0
N29-H29···O44	0.895	1.914	2.790(6)	165.7
O42-H42···N32	0.850	1.982	2.821	169.2

Table S3. Hydrogen bonding interactions in Complex 2.

D-H•••A	D-H (Å)	H•••A(Å)	D•••A(Å)	∟D-H•••A (deg)
N11-H11···O25	0.860	2.070	2.8623(18)	152.3
N9-H9···O17	0.860	1.930	2.7916(14)	178.1
O26-H26···O17	0.820	1.810	2.6179(11)	170.6

Table S4. Hydrogen bonding interactions in Complex 3.

D-H•••A	**D-H (Å)**	**H•••A(Å)**	**D•••A(Å)**	**∟D-H•••A (deg)**
O3-H3X···O2	0.820	1.770	2.593(4)	175.40
N2-H2A···O1	0.860	1.930	2.710(4)	149.90
N3-H3A···O1	0.860	2.240	2.970(4)	142.70
N3-H3B···O4	0.860	2.180	2.899(4)	140.80
N4-H4A···O2	0.860	1.920	2.741(4)	158.90

Methods.

The binding constant values of anions with **S1-S10** have been determined from the absorption data following the modified Benesi–Hildebrand equation.

$1/\Delta A = 1/\Delta A_{max} + (1/K[Anion])(1/\Delta A_{max})$.

Here, $\Delta A = A - A_{min}$, $\Delta A_{max} = A_{max} - A_{min}$.

Where, A_{min}, A, A_{max} are the absorbtion of **S1-S10** considered in the absence of anions , at an intermediate, and at a concentration of complete concentration.

K is Binding constant, [Anion] is concentration of anion .

From the Plot of $(A_{max} - A_{min.})/(A - A_{min})$ against [Anion] for **S1-S10,** the value of K ($\pm$10%) extracted from the slope.

References

(1) (a) SAINT and *XPREP*, 5.1 ed.; Siemens Industrial Automation Inc.: Madison, WI, 1995.Sheldrick, G. M. (b) *SADABS, empirical absorption Correction Program*; University of Göttingen: Göttingen, Germany, 1997.

(2) Sheldrick, G. M. *SHELXTL Reference Manual:* V*ersion 5.1*; Bruker AXS: Madison, WI, 1997.

(3) Sheldrick, G. M. *SHELXL-97: Program for Crystal Structure Refinement*; University of Göttingen: Göttingen, Germany, 1997.

(4) Spek, A. L. *PLATON-97*; University of Utrecht: Utrecht, The Netherlands, 1997.

(5) Mercury 2.2 supplied with Cambridge Structural Database, CCDC, Cambridge, UK.